Zirconium-induced physiological and biochemical responses in two genotypes
of *Brassica napus* L.

Ryan Braaf

UNIVERSITY *of the*
WESTERN CAPE

**A mini-thesis submitted in partial fulfilment of the requirements for the
degree of Magister Scientiae in the Department of Biotechnology,
University of the Western Cape.**

Supervisor: Dr. Marshall Keyster

UNIVERSITY *of the*
WESTERN CAPE

FACULTY OF NATURAL SCIENCE

PLAGIARISM DECLARATION

Name: … …………………..

Student number: …………………

1. I hereby declare that I know what plagiarism entails, namely to use another's work and to present it as my own without attributing the sources in the correct way. (Refer to University Calendar part 1 for definition)
2. I know that plagiarism is a punishable offence because it constitutes theft.
3. I understand the plagiarism policy of the Faculty of Natural Science of the University of the Western Cape.
4. I know what the consequences will be if I plagiarize in any of the assignments for my course.
5. I declare therefore that all work presented by me for every aspect of my course, will be my own, and where I have made use of another's work, I will attribute the source in the correct way.
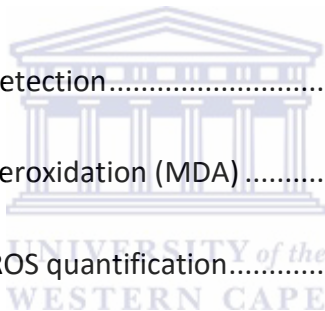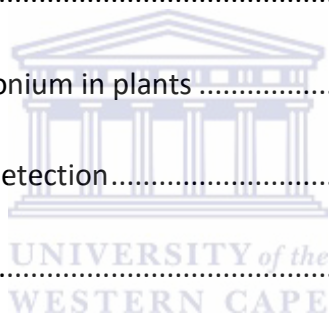
Signature   Date

-------------------------------   ----------------------

Contents

Acknowledgments

Thank you to my supervisor **Dr M Keyster** for giving me the opportunity to work in his lab. He's expertise and guidance was much appreciated as I learned so much from working on this project with him.

I would like to thank **DST** for the funding that was granted to me. It gave me a huge boost in pursuing my goals and for that I will be forever grateful.

A huge thank you to my parents **Adam Braaf and Patricia Braaf** for always encouraging me through all the rough times. Their calming and wise words through the good and the bad times have kept me grounded. Thank you for also allowing me the opportunity to follow my dreams, wherever they may lead me.
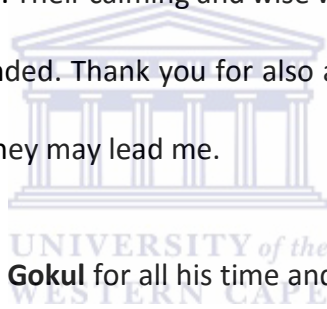
I would also like to thank **Arun Gokul** for all his time and efforts he put into helping me and giving me advice when I needed it most. I have undoubtedly learned so much from him.

A big thank you to the rest of my lab mates, **Zaahira Omar** in particular, for always being there to take my mind off my work, just enough to keep me sane. Our random conversations and lunch breaks was definitely valuble in my success.

List of abbreviations

$^1O_2$	singlet oxygen
APX	ascorbate peroxidase
As	arsenic
AS	ascorbate
ASA	ascorbate acid
cAPX	cytosolic APX
CAT	catalase
Cd	cadmium
Cr	chromium
Cu	copper
DHA	dehydroascorbate
DHLA	dihydrolipoic acid
ECR	eriochrome cyanine R
EDTA	ethylenediaminetetraacetic acid
Fe	iron
gmAPX	glyoxisome APX
GSH	glutathione peroxidase
KCN	potassium cyanide
KI	potassium iodide
MDA	malondialdehyde
Mn	manganese
MPA	mercaptopropionic acid
NADPH	nicotineamide adenine dinucleotide phosphate

NBT	nitroblue tetrazolium
Ni	nickel
PAGE	polyacrylamide gel electrophoresis
Pb	Lead
PL	Photoluminescence
PVP	polyvinylpyrrolidone
QDs	quantum dots
ROS	reactive oxygen species
sAPX	chloroplast stromal soluble APX
SDS	sodium dodecyl sulfate
SOD	superoxide dismutase
TBA	thiobarbituric acid
TCA	trichloroacetic acid
TEA	triethanolamine
TEM	transmission electron microscopy
TEMED	N,N,N',N'-Tetramethylethylenediamine
tAPX	thylakoid APX
TOPO	trioctylphosphine oxide
Zn	Zinc
Zr	zirconium

List of Figures

Chapter 1

Chapter 3

Chapter 4

Supplementary Data

List of Tables

Chapter 1

Chapter 3

Chapter 4

Supplementary Data

Abstract

South Africa is one of two countries responsible for the production of approximately 80% of the world's Zr. The increase in mining activity has detrimental effects on the environment, especially crop plants, as more pollutants are leached into the soil. Consequently, it is necessary to understand how plants respond to this form of abiotic stress. Therefore, this study focused on determining the physiological and biochemical responses of two genotypes of *Brassica napus* L (Agamax and Garnet) in response to Zr stress. The levels of cell death, lipid peroxidation and ROS were higher in Garnet, whereas the chlorophyll content was higher in Agamax. Furthermore, native PAGE analysis detected seven SOD isoforms and seven APX isoforms in Agamax, compared to 6 SOD isoforms and 7 APX isoforms in Garnet. The results thus indicate that Agamax is tolerant to Zr-induced stress, whereas Garnet is sensitive. An assay for the rapid quantification of Zr within plant samples was subsequently developed, which revealed that Agamax retained the bulk of the Zr within its roots, whereas Garnet translocated most of the Zr to its leaves. The ability of Agamax to sequester Zr in its roots comes forth as one of the mechanisms which confers greater tolerance to Zr-induced stress. As a consequence, our study sought to use the optical, physical and chemical properties of quantum dots to image the uptake and translocation of Zr in *B. napus* genotypes. ICP-OES was also performed to quantify Zr levels in various plant organs. Data from the ICP-OES revealed varying patterns of uptake and translocations between Garnet and Agamax. These patterns were similarly shown in IVIS Lumina images, tracing the transport of QD/Zr conjugates. This method ultimately proved to be successful in tracing

the uptake of Zr, and could essentially be a useful tool for targeting and imaging a number of other molecules.

Chapter 1

Literature Review

1.1.   Introduction

South Africa is one of the most important countries in terms of the wide selection of minerals they produce (eg. gold, vanadium, zirconium, etc.), not only in Africa, but also worldwide (Erasmus, 2013). It generates an estimated R23-trillion from mineral sales and has the world's largest reserves of gold (Au), chromium (Cr), manganese (Mn) and the second-largest reserves of vanadium (V) and zirconium (Zr). South Africa is one of two countries that produce 80% of the world's Zr (Emsley, 2001). The mining industry is therefore the main driving force behind the South African economy. However, zirconium production may have detrimental effects on the environment (Abdul-Wahab and Marikar, 2012; McCarthy, 2011). These effects are brought about by the fact that heavy metals are toxic to plants, and therefore induce stress (Schützendübel and Polle, 2002).

This form of stress is known as abiotic stress and is currently of great concern globally as it is responsible for the loss of more than 50% of crop plants (Wang *et al*., 2003). These stresses result in the deterioration of the environment and include conditions such as salinity, drought, extreme temperatures, chemical toxicity and heavy metal toxicity. Thus, the growth and productivity of plants is negatively affected as they undergo a number of morphological, biochemical, physiological and molecular changes (Wang *et al*., 2003). As a consequence of the sessile nature of plants, they are continuously

exposed to these environmental conditions, and have therefore evolved a diverse set of protective mechanisms (Ciarmiello *et al.*, 2011; Vickers *et al.*, 2009).

Depending on the type of stress, plants are able to respond instantaneously to changes in the environmental conditions (Ciarmiello *et al.*, 2011). Under abiotic stress, plants prompt for suitable responses, by altering their metabolism, growth and development. They achieve this by various regulatory mechanisms such as stress sensors, signalling pathways consisting of a number of protein-protein interactions, transcription factors and promoters and ultimately the production of specific proteins or metabolites (Ciarmiello *et al.*, 2011). One of the most important pathways involved in alleviating stress in plants is the antioxidant-ROS pathway. Studies have shown that plants overproduce reactive oxygen species (ROS) via this pathway when it experiences these stress conditions (Shao *et al.*, 2008; Fodor *et al.*, 2005).
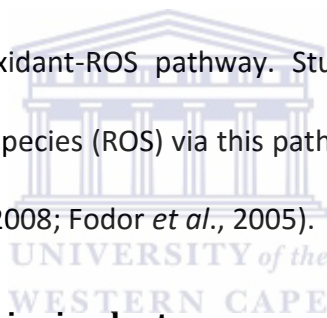
1.2. Reactive oxygen species in plants

Various heavy metals, including Zr, at different concentrations have the ability to signal the production of ROS in more than one particular way; directly through Haber-Weiss reactions or indirectly as a consequence of oxidative stress caused by heavy metal toxicity (Yadav, 2010; Gratão *et al.*, 2005; Wojtaszek, 1997). ROS are said to be the toxic by-products of a plant's natural aerobic metabolism and are also found to play a crucial role in signalling and control various processes such as development, growth, response to biotic and abiotic environmental stimuli and programmed cell death (Bailey-Serres and Mittler, 2006; Apel and Hirt, 2004). These molecules are produced in several compartments in the cell, including the plastids, chloroplasts, mitochondria, apoplast,

cytosol and peroxisomes. Figure 1 suggests that ROS production and accumulation can also initiate signalling cascades under normal conditions (Shao *et al*., 2008; Van Breusegem and Dat, 2006). ROS in plants occur in four main forms; hydrogen peroxide (H_2O_2), superoxide anion (O_2^-), hydroxyl radical ($OH\bullet$) and singlet oxygen ($^1O_2$), and these can all lead to oxidative damage of cells. However, according to Gough and Cotter (2011), H_2O_2, O_2^- and $OH\bullet$ have been the focal point of recent research.
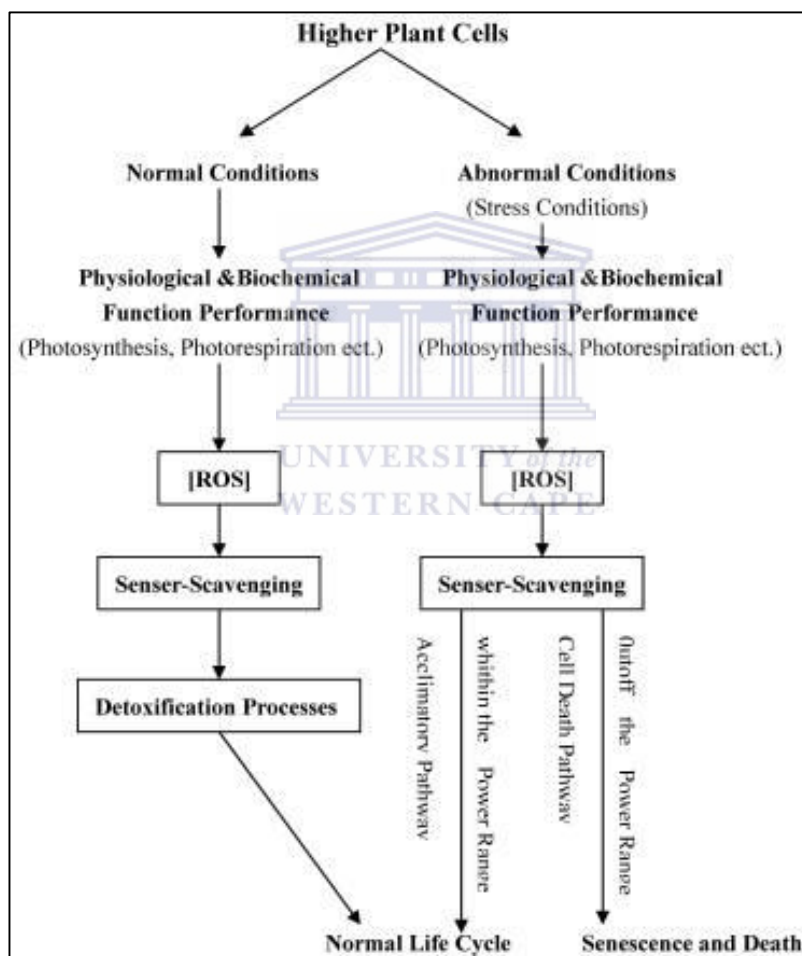
Figure 1: Two distinct signalling cascades plant cells may undergo; during normal and stressed conditions (Adopted from Shao *et al*., 2008).

1.2.1. Hydrogen peroxide (H_2O_2)

H_2O_2 is a univalent reduction product of O_2^- that is theoretically reactive; however, it is not a free radical (Cheeseman, 2007). Therefore, H_2O_2 is relatively harmless when compared to O_2^-, and is only reactive in the presence of transition metals; otherwise it is quite stable even at very high concentrations (Cheeseman, 2007; Halliwell *et al.*, 2000). H_2O_2 molecules are produced by various cellular reactions which include the Fenton reaction, as well as a number of enzymes such as nicotinamide adenine dinucleotide phosphate (NADPH) oxidase, peroxidase and xanthine oxidase (Blokhina *et al.*, 2003). A number of studies suggest that in plant cells, where transition metals are crucial in the growth and development of plants, high levels of H_2O_2 display damaging effects to cells by fragmenting DNA and oxidizing lipids (Gough and Cotter, 2011; Hall and Williams, 2003).
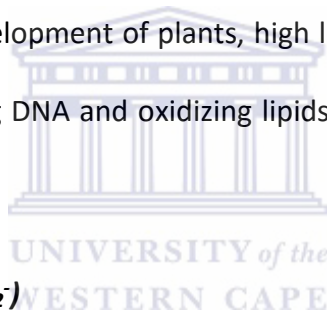
1.2.2. Superoxide radicals (O_2^-)

The superoxide anion is a one-electron reduction of oxygen (O_2) and it is moderately reactive (Turrens, 2003; Puntarulo *et al.*, 1988). These ions are formed primarily in the chloroplast during photosynthesis, where the oxygen produced can accept electrons transporting them through the photosystems and therefore forming O_2^- (Gill and Tuteja, 2010). Like H_2O_2, O_2^- is similarly produced by the same reactions and enzymatic mechanisms that are present in the cell (Blokhina *et al.*, 2003). The main site of O_2^- generation within the chloroplast is the primary electron acceptor of Photosystem I (PSI) in the thylakoid membrane. It is suggested that approximately 1-2% of O_2 consumed in plant cells results in the production of O_2^- (Gill and Tuteja, 2010; Puntarulo *et al.*, 1988). As a consequence, more ROS like OH• can be generated, which can ultimately lead to

lipid peroxidation of membranes and the weakening of the cell structure (Gill and Tuteja, 2010; Halliwell, 2006).

1.2.3. Hydroxyl radical (OH•)

Hydroxyl radicals (OH•) are one of the most reactive ROS molecules that exist and can be created from O_2^- and H_2O_2 in the presence of particular transition metals such as iron (Fe) (Gill and Tuteja, 2010; Babbs *et al.*, 1989). This reaction catalysed by Fe occurs at ambient temperatures and neutral pH, and is mediated by O_2^-; essentially known as the Fenton reaction (Gill and Tuteja, 2010).

$$H_2O_2 + O_2^- \xrightarrow{\text{Fe}^{2+}, \text{Fe}^{3+}} OH^- + O_2 + OH•$$
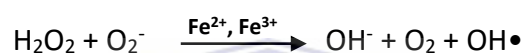
These molecules can practically react with any macromolecule it comes across, including membrane lipids, proteins and DNA. Studies have thus shown that insufficient scavenging of excess OH• may cause cell death and ultimately the death of the plant (Gill and Tuteja, 2010; Vranova *et al.*, 2002).

All these molecules have been shown to have damaging effects on plants. However, there are a number of ways in which plants can remove these toxic products, and one well-understood technique is through the antioxidant system (Bailey-Serres and Mittler, 2006; Apel and Hirt, 2004, Blokhina *et al.*, 2003). Previous studies suggest that the most common antioxidant enzymes found in plants are ascorbate peroxidase (APX), superoxide dismutase (SOD) and catalase (CAT). However, other non-enzymatic antioxidants also exist, such as ascorbic acid (ASA) and glutathione (GSH) (Sharma and Dietz, 2008).

5

1.3. ROS scavenging antioxidant enzymes and other antioxidant compounds in plants

1.3.1. *Superoxide dismutase*

Superoxide dismutase (SOD) is thought to be the primary mechanism of defence against ROS in a cell (Shahab Jalali-e-Emam *et al*., 2011; Elstner, 1991). SODs catalyse the dismutation of O_2^-, one being reduced and another oxidized to H_2O_2 and O_2 respectively (Table 1). The reduction of O_2 to form O_2^- can occur in various parts of the cell because it essentially requires an electron transport chain for its production and partly due to enzymatic activity. The main compartments involved in O_2^- generation include the mitochondria, chloroplast and the peroxisomes (Sharma *et* al., 2012; Fridovich, 1986). It is important to note that phospholipid membranes are impermeable to O_2^- molecules, and thus SODs play a vital role in the removal of these radicals (Myouga *et al*., 2008; Takahashi and Asada, 1983). There are 3 types of SODs, which are essentially classified in relation to their metal co-factor used in each of these enzymes: manganese SOD (Mn SOD), iron SOD (Fe SOD) and copper-zinc SOD (Cu-Zn SOD). Each SOD is characteristically located in various compartments within the cell (Figure 2); Mn SODs being located in the mitochondrion and peroxisome, Fe SODs in the chloroplast, and Cu-Zn SODs in the chloroplast, cytosol and extracellular space (Kuo *et* al., 2013; Miriyala *et al*., 2012; Alscher *et al*., 2002). A study has shown the presence of these enzymes in plants of the *Brassica* family; however, little is known about their presence in canola under Zr-induced oxidative stress (Shahab Jalali-e-Emam *et al*., 2011).
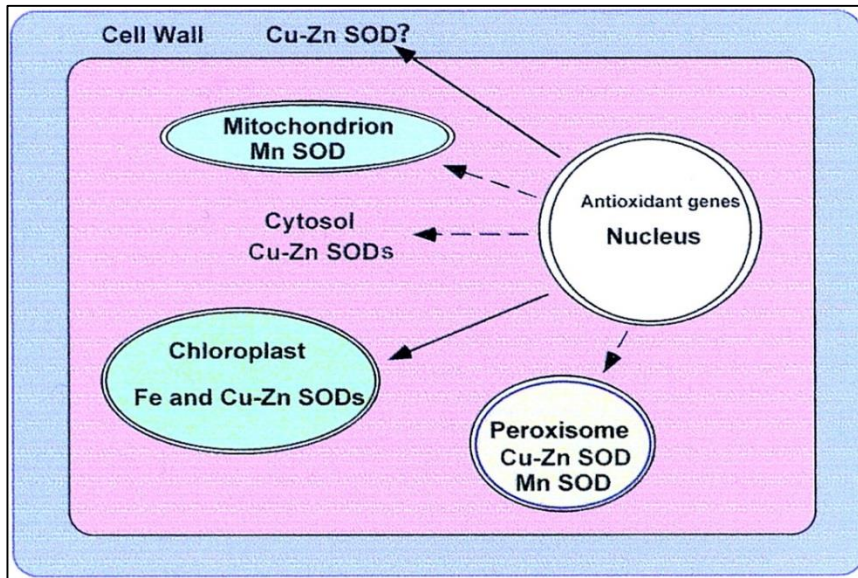
Figure 2: Respective locations of each SOD within a cell (Adopted from Alscher *et al*., 2002).

A variety of SOD genes have been identified in several plant species, such as *Arabidopsis thaliana*, *Medicago truncatula* and *Brassica juncea* (Koramutla *et al*., 2014; Gill and Tuteja, 2010; López-Millán *et al*., 2005). These enzymes are characterised by their sensitivity to various molecules. Fe SOD can be inactivated by H_2O_2, but is resistant to inhibition by potassium cyanide (KCN). This is key in distinguishing between various SOD enzymes (Alscher *et al*., 2002). Unlike Fe SODs, it was shown that Cu/Zn SODs are inhibited by KCN (Cohu and Pilon, 2007). Contrastingly, Mn SODs are neither sensitive to H_2O_2, nor KCN, however, a study done by Brou *et al* (2007) has shown the inhibition of Mn SODs by 2% SDS, thus making it possible to distinguish between Fe and Cu-Zn SODs.

1.3.2. Ascorbate peroxidase (APX)

In higher plants, APX is said to play an essential role in ROS scavenging. APX is a well-known group of antioxidant enzymes which consist of 5 isoforms; cytosolic form (cAPX),

7

chloroplast stromal soluble (sAPX), glyoxisome membrane (gmAPX), and thylakoid (tAPX) (Gill and Tuteja, 2010). The APX family of enzymes all function by scavenging H_2O_2 and it uses ASA as an electron donor in this process, to produce water and dehydroascorbate (DHA) (Table 1). An important characteristic of APX is that in the absence of ASA, these enzymes are quite unstable. A study has shown that at ASA concentrations below 20 μM, the activity of APX is lost fairly quickly (Noctor and Foyer, 1998). According to Badawi and colleagues (2004), APX production is exhibited in plants under a number of different abiotic stresses and in some cases, the overexpression of this enzyme seems to have improved the tolerance of the plant toward the specific stress. Other studies suggest that an increase in heavy metal concentrations beyond their respective thresholds may simultaneously increase the activity of various antioxidant enzymes such as APX and CAT (Gough and Cotter, 2011).
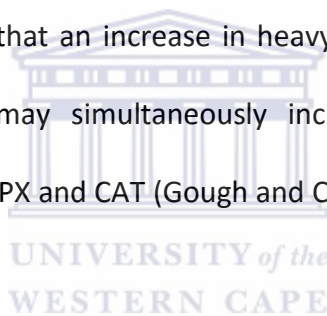
1.3.3. Catalase (CAT)

CAT is a tetrameric, iron-containing protein that functions by catalyzing the conversion of H_2O_2 to a water molecule and oxygen (Table 1). This enzyme is unique when compared to other antioxidant enzymes as it does not require a reductant for the disproportionation reaction, as it accomplishes this all on its own (Mhamdi *et al.*, 2010; Garg and Manchanda, 2009). CAT is fundamental in protecting cells against the damaging effects of ROS, especially by eradicating H_2O_2 found in the peroxisomes as a result of oxidases involved in photorespiration, β-oxidation of fatty acids and purine catabolism. This is evident as CAT has one of the highest turnover number of all the antioxidant enzymes; it can convert approximately 6 million molecules of H_2O_2 to H_2O and O_2 per minute (Gill and Tuteja, 2010; Mhamdi *et al.*, 2010). Studies have shown that

CAT isoforms have been found in plants; however, knowledge about its subcellular localization is lacking. It has however been established that CAT isoforms, as a consequence of heavy metal stress, contribute to improved seedling growth and longer roots in *B. juncea* (Gill and Tuteja, 2010; Gichner *et al*., 2004).

Table 1: Various antioxidant enzymes together with their respective reactions which they catalyze (Adapted from Gill and Tuteja, 2010).

Enzymatic antioxidants	Enzyme code	Reaction Catalyzed
Superoxide dismutase	EC 1.15.1.1	$O_2^- + O_2^- + 2H^+ \longrightarrow 2H_2O_2 + O_2$
Ascorbate peroxidase	EC 1.11.1.11	$H_2O_2 + ASA \longrightarrow 2H_2O + DHA$
Catalase	EC 1.11.1.6	$H_2O_2 \longrightarrow H_2O + {}^1\!/_2 O_2$

1.3.4. Ascorbic acid (Vitamin C)

ASA is a water-soluble antioxidant that functions by relieving the effects of ROS in plant cells (Foyer and Noctor, 2011; Smirnoff, 2005). Furthermore it acts as a free radical scavenger, a reducing agent and an enzyme cofactor (Montecinos *et al*., 2007). It is considered to be the most abundant and potent non-enzymatic antioxidant that exists and can be found throughout all plant tissues. It is especially copious in photosynthetic cells and meristems. The highest concentration of ASA was shown in mature leaves, where the chloroplasts are completely developed and chlorophyll content is at its peak (Gill and Tuteja 2010**;** Smirnoff, 2000). The main source of ASA production in plant cells is the mitochondrion and approximately 35% of ASA in the cell is at a concentration of 50 mM (Foyer and Noctor, 2005).

1.3.5. Glutathione (GSH)

Glutathione is a water-soluble, sulfhydryl (-SH) antioxidant and enzyme cofactor. It is ubiquitous in plant cells; typically abundant in aqueous phases of the cell such as the cytosol, endoplasmic reticulum, mitochondria, chloroplasts, peroxisomes, apoplast and the vacuole (Gill and Tuteja, 2010; Jimenez *et al*., 1998; Mittler and Zilinskas, 1992). In addition, GSH also plays a crucial role in numerous physiological processes such as expression of stress-response genes, sulphate transport, conjugation of metabolites, detoxification of xenobiotics and redox balance (Figure 3) (Noctor *et al*., 2012; Mullineaux and Rausch, 2005; Xiang *et al*., 2001). These studies have also confirmed that GSH is involved in the growth and development of plant processes such as cell death and senescence. One of the most essential roles of GSH in the antioxidant defence system is its ROS scavenging ability and also its ability to regenerate ASA from its oxidized forms by the ASA-GSH cycle.
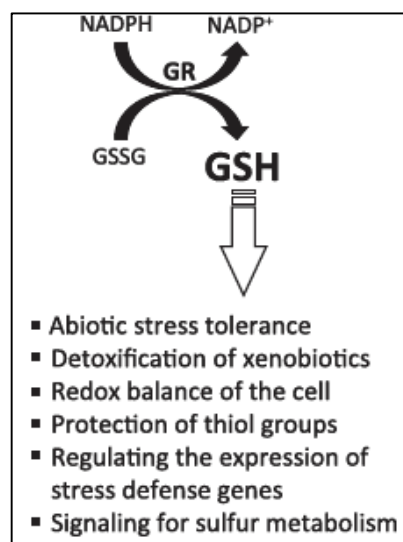
Figure 3: Role of glutathione in plant metabolism (Adopted from Gill and Tuteja, 2010).

1.4. Damaging effects of ROS on plant cells

1.4.1. Lipid peroxidation

Lipid peroxidation is the process by which the polyunsaturated fatty acids of the cell membrane are attacked by ROS molecules, which induces a self-propagating chain reaction (Thanan *et al*., 2015; Mylonas and Kouretas, 1999). This oxidative destruction is essentially brought about by the removal of electrons from the lipids in the cell membrane, which ultimately alters its permeability and fluidity (Barrera, 2012; Gill and Tuteja, 2010; Marnett, 1999). This reaction occurs only when the ROS threshold of a cell has exceeded that of the antioxidants. The key end products of lipid peroxidation include ketones, malondialdehyde (MDA) and other associated compounds, therefore making these molecules important indicators of lipid peroxidation in plant cells (Garg and Manchanda, 2009). The product MDA is particularly important as it can interact with thiobarbituric acid (TBA) to form a coloured end product called TBA reactive substances, and as a consequence makes it possible to analyse the extent of lipid peroxidation in a cell (Gill and Tuteja, 2010).

1.4.2. DNA damage

The genome of a plant is highly stable; however, DNA damage may occur when it is exposed to DNA-damaging agents (Gill and Tuteja, 2010; Tuteja *et al*., 2009). A number of these agents exist which include radiation, chemical agents (eg. hydrogen peroxide and vinyl chloride). However, abiotic stress due to heavy metal toxicity causes spontaneous damage through high levels of ROS (eg. free radicals and O_2^-). ROS is said to cause damage directly to nucleic acids. The most damaging ROS is OH• as it is the

most reactive, and can destroy both purine and pyrimidine bases, as well as the deoxyribose backbone (Birben *et* al., 2012; Cooke *et al*., 2003; Halliwell and Gutteridge, 1999). H_2O_2 and O_2^- are not reactive with guanine in DNA molecules; however, $^1O_2$, an unusual form of ROS, has been associated with the destruction of these nucleobases. There are numerous ways in which ROS can damage DNA which include base modifications, strand breaks, base deletion, pyrimidine dimers and cross links (Tuteja and Tuteja, 2001; Tuteja *et al*., 2001). These damages may cause further physiological effects for example cell membrane destruction, decrease in protein synthesis, and disruption of the photosynthetic machinery, which could ultimately have an impact on the growth and development of the plant.

1.4.3. Reduction in chlorophyll production

Chlorosis is the discoloration (loss of green colour) of the leaves of a plant due to the lack of chlorophyll (Fatoba and Emem, 2008). The colour of the leaves can range from light green to yellow and in severe cases brown. Studies have shown that heavy metal toxicity contributes to this detrimental effect in plants; the higher the metal concentration, the higher the degree of chlorosis. When chlorosis reaches a certain degree, the plant eventually dies (Shakya *et* al., 2008; Brown *et al*., 1986). This effect on the plant is essentially due to the temporary inhibition of photosynthesis, increased respiration, reduction in chlorophyll *a* and *b*, and considerable loss of intracellular potassium (Shakya *et* al., 2008). Metals that are generally used in experiments of this nature include lead (Pb), cadmium (Cd), chromium (Cr), Cu, Zn and aluminium (Al). However, studies involving zirconium and its effects are few and limited.

1.4.4. Cell and tissue death

Cell and tissue death in plants is known as necrosis, and is physically visible in plants by dark watery or even dry spots (Norris, 2013; Yadav, 2010). The degree of chlorosis in plants has been shown to increase where there is an increase in heavy metal concentration. Studies suggest that this is a sign of plant-perceived stress and is said to be a direct effect a nutrient imbalance in cells or the effect of one of many plant diseases (Norris, 2013, Wong, 2006). However, similar to chlorosis, there is limited knowledge detailing the effect of Zr on necrosis; the most focus being placed on heavy metals like Cu, Zn, nickel (Ni) and Al (Yadav, 2010; Rahman *et al*., 2005). Given that a physical assessment of a plant may involve some sort of bias, studies generally use Evans blue; a non-permeable dye that has the ability to enter non-viable cells, for the measurement of cell death in both leaves and roots (Yamamoto *et al*., 2001)
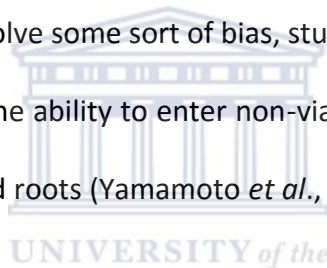
1.5. Strategic distribution of heavy metals in plants

Other than antioxidants and antioxidant enzymes, another frequent strategy employed by plants when exposed to phytotoxic levels of heavy metals is to prevent them from entering roots cells (Rascioa and Navari-Izzob, 2011; Rascio *et al*., 2008; Dalla Vecchia *et al*., 2005). This is achieved by trapping the heavy metals in the apoplast, allowing them to attach to organic acids and negatively charged groups of cell walls. However, heavy metals which manage to be taken up into the plant are retained in root cells, where they may either be removed through forming complexes with organic acids, amino acids or metal-binding proteins or isolated into vacuoles (Hall, 2002). This strategy avoids the

translation of metals to plant structures above ground, thereby protecting the leaf tissue and more specifically the photosynthetic cells from oxidative damage (Figure 4).

1.5.1. Heavy metal hyperaccumulator plants

Plants that are classified as hyperaccumulators are characteristically able to acquire enormous amounts of heavy metals from the soil, which may include a number of different metals such as Ni, Pb, Zn and Cu (Rascioa and Navari-Izzob, 2011). Furthermore, they are capable of translocating these heavy metals from the root to the leaves, in concentrations far beyond that of non-hyperaccumulators (excluders). In contrast, non-hyperaccumulating plants manage to keep the heavy metals in the roots, where they are later detoxified. The main feature of hyperaccumulators is that they display no signs of phytotoxicity (Verbruggen *et al.*, 2009; Reeves, 2006).

1.5.2. Mechanisms of metal hyperaccumulation in plants

The amount of heavy metals taken up by hyperaccumulators varies between different genera and species of plants (Rascioa and Navari-Izzob, 2011; Krämer, 2010; Deng *et al.*, 2007; Roosens *et al.*, 2003). These plants are essentially different from non-hyperaccumulators based on three characteristic principles: a more superior ability of acquiring metals from the soil; more rapid and efficient translocation of metals from roots to shoots; and an enhanced technique of isolating and detoxifying large quantities of heavy metals in the leaves (Figure 4).
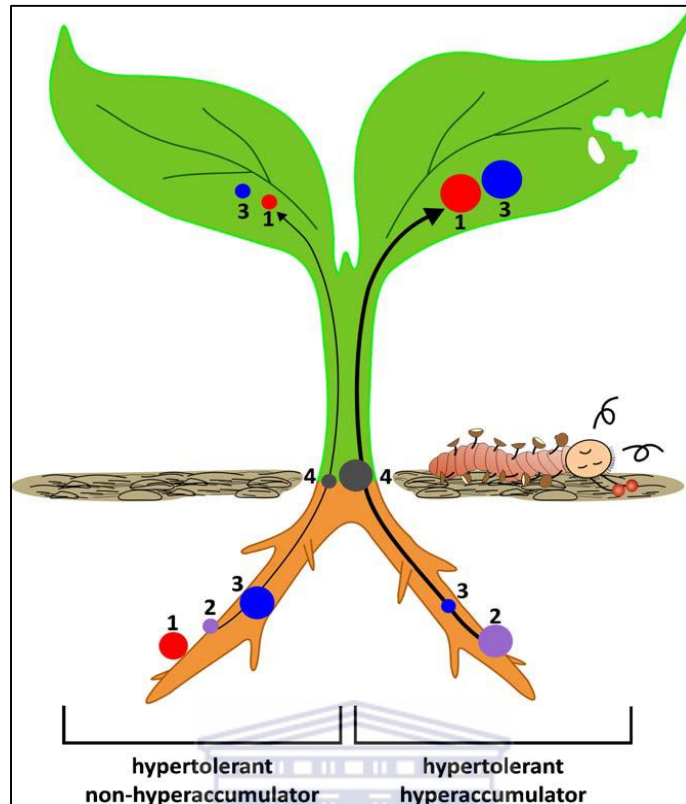
Figure 4: Different strategies in the distribution of heavy metals; non-hyperaccumulator (left) and hyperaccumulator (right). (1) Binding of heavy metal to cell walls, (2) uptake in the roots, (3) formation of complexes in root cells and or isolation in vacuoles, (4) translocation from roots to shoots. The spots represent the location (tissue) wherein these mechanisms take place and are proportional, in terms of size, to their respective amounts retained (Adopted from Rascioa and Navari-Izzob, 2011).

Hyperaccumulators have been studied extensively over the last few years and have been comprehensively compared to non-hyperaccumulators. Verbruggen *et al* (2009) suggests that the genes involved in hyperacculmulation are not exclusive to hyperaccumulator species. In fact, they share mutual genes. The only difference is that these genes are differentially expressed and regulated in hyperaccumulators.

15

1.6. Nanotechnology: How it's unique properties can be exploited for *in vivo* imaging

Nanotechnology refers to the science of creating and manufacturing of machines, devices and systems that encompass the unique physical, chemical, optical and biological properties of particles by altering its shape and size at the nanometer scale (Ebbesen and Jensen, 2006). As a result, nanoparticles have therefore become a tool of great promise for targeting and imaging (Hild *et al*., 2008). A number of nanoparticles are capable of targeting various molecules, such as colloidal gold and superparamagnetic iron oxide particles. However, the ideal nanoparticles for simultaneous targeting and imaging are quantum dots (QDs). This is mainly due to their unique optical properties, which is attributed to that of the quantum confinement effects of their size and structure at the nanoscale (Shi *et al*., 2015)

One useful characteristic of any nanoparticle is that it can be used as carrier molecules, which can be used to transport (direct or passive) molecules (Rana *et al*., 2012). This can either be done by incorporating the molecule in the nanoparticle, or attaching it to its surface by means of various linkers or chemical routes which include adsorption, electrostatic interaction, mercapto (-SH) exchange, and covalent linkages (Ghosh *et al*., 2008; Alivisatos *et al*., 2005). A study done by Cai *et al* (2006) provides an example of simultaneous targeting and imaging of a tumour in mice; using arginine-glycine-aspartic acid (RGD) peptide as the targeting ligand and the optical properties of QDs for *in vivo (*cellular and intracellular) imaging (Hild *et al*., 2008). However, QDs are quite toxic and would consequently not be ideal for use when working with live cells and animals. Studies have therefore negated this problem by capping the hydrophobic quantum dot

with hydrophilic molecules such as dihydrolipoic acid (DHLA) and mercaptopropionic acid (MPA) (Yu *et al.*, 2012; Mattoussi *et al.*, 2001; Mattoussi *et al.*, 2000).

Once the synthesis of any nanoparticle is complete, it needs to be validated to determine whether the desired result was achieved. There are several techniques that are used to characterize nanoparticles, however the methods used for characterization of a particular nanoparticle is determined by what information is required. The most typical characterization methods used are photoluminescense spectroscopy, UV-visible spectroscopy, scanning electron microscopy, transmission electron microscopy and dynamic light scattering; each of them providing vastly different analyses of a particular nanoparticle (Hild *et al.*, 2008; Choi *et al.*, 2007).
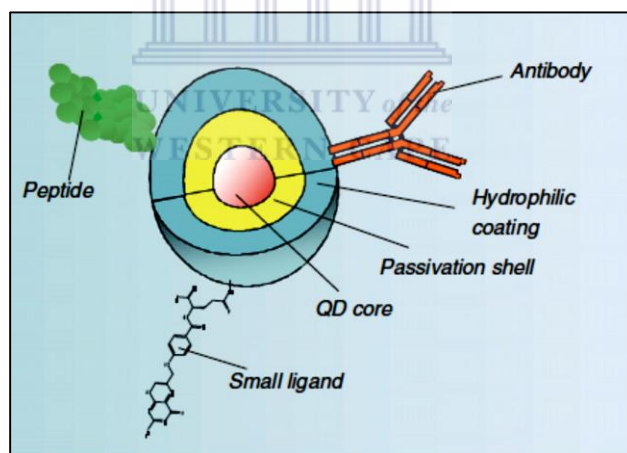
Figure 5: Illustration of a typical core-shell nanoparticle (quantum dot) prepared for biological applications. It consists of a semiconducting nanocrystal core, coated by another semiconductor shell. To make this molecule suitable for conjugation to biologically active molecules (eg. antibody, peptide and small ligands) and less toxic, the entire surface of the quantum dot is covered by a hydrophilic coating (Alivisatos *et al.*, 2005). The biologically active molecules that are subsequently attached are used to target specific biological molecules.

1.7.   Conclusion

Mining activity in South Africa plays a crucial role in soil contamination and in turn affects crop yield and production. Heavy metal toxicity, which is a form of abiotic stress, consequently leads to the production of high levels of various ROS which include H_2O_2, O_2^-, $^1O_2$ and OH•. These high levels of ROS may lead to oxidative damage of plant cells, and eventually death of the cells and the organism. Plants however have defensive mechanisms in place to eliminate detrimental effects of these molecules. They produce antioxidant enzymes such as SOD, APX and CAT in different compartments of the cells, and these enzymes aid in the scavenging of ROS molecules. Plants also produce antioxidants such as ASA and GSH to help alleviate the phytotoxic effect of heavy metals. Although strategies are in place to deal with heavy metals in the soil, plants are still negatively affected by elevated levels of heavy metals.
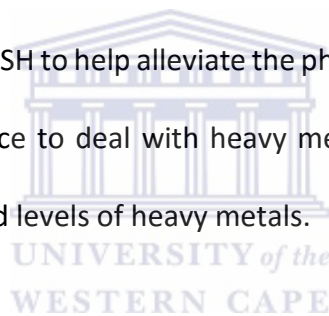
1.8.   Justification

In crop producing countries which are incessantly affected by environmental changes such as drought, salinity of soils and an increase in mining activity, it is crucial to understand the pathways that may cause the destruction of plant cells and eventually the death of the entire plant (Yadav, 2010). One of these countries include South Africa, which is experiencing a continuous decrease in cultivable land (Mohamed, 2000). It was estimated that approximately 13.5% of the land is appropriate for the production of crops, and furthermore only 3% of this land is considered as greatly potential land. With the ever increasing population in South Africa, and thereby a greater demand for food production, full use should be made of the available land (Blaine, 2012). However, a total

of 6% of this land is used for mining, which ultimately makes this an insurmountable task (Palmer and Ainslie, 2006).

1.9. Aims and Objectives

- Identify heavy metal sensitive and tolerant genotypes of *B. napus* by measuring phenotypic characteristics, conducting visual examinations and determine the levels of cell death.

- Develop a spectrophotometric assay for quantifying zirconium for the rapid quantification of the metal in the roots and shoots of two plant genotypes.

- Identify enzymes involved in tolerance to heavy metal stress, such as SOD and APX. In addition, quantify lipid peroxidation and various ROS molecules.

- Confirm studies for the quantification of Zr will be conducted by inductively coupled plasma optical emission spectrometry (ICP-OES).

- Synthesis of water-soluble CdTe/ZnS QDs for visualising the uptake and translocation of Zr in *B. napus*.

1.10. Highlights

- Two genotypes of *B. napus* were selected, of which Garnet displayed higher levels of cell death, lipid peroxidation and ROS compared to Agamax.

- Agamax displayed higher levels of chlorophyll content compared to Garnet.

- Agamax revealed seven isoforms for both SOD and APX, whereas Garnet expressed six and seven isoforms of SOD and APX respectively.

- A Zr assay for plants showed that Agamax retains most of the Zr in its roots, while Garnet translocates the metal to its leaves.

- The data suggested that Agamax is tolerant to stress induced by Zr, whereas Garnet was shown to be sensitive.

- The aforementioned work was presented at a conference

  Ryan Braaf, Marshall Keyster (2014) Zirconium-induced stress responses in two contrasting *Brassica napus* L. genoptypes. The 24th biennial congress of the South African Society of Biochemistry and Molecular Biology (SASBMB), ATKV Goudini spa, Rawsonville, **South Africa**.

- ICP confirmed data displayed by the Zr assay.

- Water-soluble CdTe/ZnS quantum dots were successfully synthesised.

- QDs were conjugated with Zr, and subsequently imaged *in vivo* within both *B. napus* L genotypes.

- Images generated by the IVIS Lumina imaging system similarly revealed the same pattern of Zr translocation in Agamax and Garnet to that observed in the Zr quantifications.
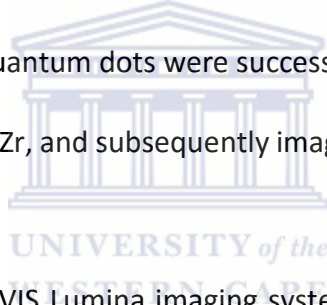
Chapter 2

Materials and Methods

2.1. Plant growth and treatment

Three sets of soil mixtures containing a ratio of 3:1 of soil and filter sand respectively, were prepared. Each set of soil mixture was pre-treated with a different solution prior to sowing the seeds; untreated control (water), 500 µM $ZrCl_4$, and 1 mM $ZrCl_4$. The seeds of two canola (*Brassica napus* L) genotypes; Agamax and Garnet, were subsequently sown in each of these pre-treated soil mixtures and supplemented with their respective treatments every 3 days during germination. Following germination, each seedling was placed into separate pots (1 per pot) and the treatment thereof continued for a period of 28 days. This was done as an initial test to determine the optimum concentration of Zr which would induce the ideal amount of stress within the plant. The concentration selected to carry out further experiments was 1 mM Zr.

The seeds of both genotypes of canola plants were sown as previously described. Pre-treatment and treatment was carried out using water until the mature growth stage was reached (4 leaf stage). Thereafter, each plant was treated with 1 mM Zr every 3 days, for a total of 28 days. Simultaneously, a control set of plants were grown for the same time period using water.

Growth parameters (leaf and root morphology, biomass), cell viability, chlorophyll content, MDA content, ROS (O_2^- and H_2O_2) levels, antioxidant enzyme (SOD and APX) activities, and Zr levels were evaluated. For the evaluation of growth parameters,

superoxide content and cell viability, freshly harvested plants were used. For the rest of the assays, snap-frozen ground leaf material (in liquid nitrogen) was used which was stored at -80°C.

2.2. Growth Parameters

For the analysis of leaf and root morphology, the leaves and roots of both genotypes were separated and measured alongside their respective controls. For the determination of biomass, leaves and roots were placed in an oven at 65°C for 48 hours. The dry weights were measured to determine its biomass.

2.3. Extraction of proteins

Proteins were extracted from the leaves of untreated and Zr-treated plants for subsequent use in the activity analysis in native PAGE. A triple extraction of the protein from each sample was accomplished by adding 100 mg of frozen leaf material into three Eppendorf tubes respectively. Into one of the three tubes from each sample, 500 µl of phosphate extraction buffer (40 mM phosphate buffer, 1 mM EDTA and 5% PVP) was added. Each of these mixtures was mixed vigorously using a vortex. The plant material was pelleted in a centrifuge at 13000 x g for 5 minutes and the subsequent supernatant was transferred into the second tube containing 100 mg of frozen ground plant material. The previous steps were repeated for tubes 2 and 3. A clean tube was used for the transferral of the supernatant from the third tube, which was subsequently used for quantification using a Bradford assay. These protein samples were stored at -20°C.
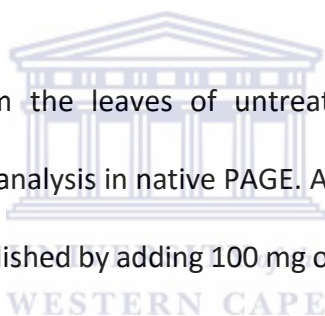
2.4. Determination of protein concentration

The concentration of the extracted proteins was determined as specified by the manufacturer of Bio-Rad 1x Bradford's reagent.

2.5. Antioxidant isoform detection

For the separation of SOD and APX isoenzymes, 200 µg of protein mixed with 4x orange G loading dye was subjected to native PAGE; 5% stacking and 13% resolving gels under constant voltage (60V) at 4°C, for 4 hours. Thereafter, the gels were washed with water before conducting the subsequent incubation steps. All the incubations were carried out in the absence of light, at room temperature.

For the visualization of SOD isoforms, the first incubation was done by submerging the gel in a 50 mM phosphate buffer solution (pH 7.0) for 20 minutes, while shaking. After the allotted time, the solution was discarded, and the gel was incubated in a second 50 mM phosphate buffer (pH 7.8) solution containing 0.5 mM NBT. It was shaken for 20 minutes, where-after the solution was discarded. The next incubation step was done in 50 mM phosphate buffer (pH 7.8) containing 35.5 mM TEMED and 0.5 mM riboflavin. Another incubation period of 20 minutes was allowed, while shaking. The solution was then discarded, and subsequently exposed to light for the visualization of SOD activity.

For the visualisation of APX isoforms, the gels were initially equilibrated in native PAGE running buffer containing 2 mM ascorbic acid, for 30 minutes at 4°C, prior to the addition of the samples onto the gel. Following the previously described protein separation method, the gels were incubated in three different solutions. The first incubation step was performed by immersing the gel in a 50 mM phosphate buffer solution (pH 7.0)

containing 2 mM ascorbic acid. An incubation time of 20 minutes was allowed, while

shaking. Once the incubation period was over, the solution was discarded, and this was

followed by the second incubation in 50 mM phosphate buffer so (pH 7.8) containing 4

mM ascorbic acid and 2 mM H_2O_2. Another incubation period of 20 minutes was

allowed, while shaking. The solution was discarded, and was followed by the addition of

the third solution of 50 mM phosphate buffer containing 28 mM TEMED and 0.5 mM

NBT. After another 20 minutes of incubation, the solution was discarded. The

subsequent visualization of the isoenzymes was done by exposing the gel to light.

2.6. TBARS assay of lipid peroxidation (MDA)

The level of lipid peroxidation was estimated according to Seckin *et al* (2010), however,

a few amendments were made. The analysis was done by measuring the amount of one

of its low-molecular weight end products known as MDA. Homogenization of 100 mg of

shoot material was done in 6% trichloroacetic acid (TCA). The solution was centrifuged

at 13000 x g for 10 minutes and to 200 µl of the subsequent supernatant, 300 µl of 0.5%

TBA in 20% TCA was added. The mixture was heated at 95°C for 20 minutes, followed by

the termination of the reaction on ice for 10 minutes. Thereafter, the mixture was

centrifuged at 13000 x g for 5 minutes and the absorbance was recorded at 532 and 600

nm. Before ultimately determining the MDA concentration from the extinction

coefficient of 155 mM^{-1} cm^{-1}, the nonspecific turbidity was subtracted at 600 nm.

2.7. Spectrophotometric ROS quantification

The determination of O_2^- was done as previously described by Russo *et al* (2008)

however, a few amendments were made. Fresh leaf discs (1 cm^3) and roots (2 cm from

the tip) were cut respectively for each treatment, masses recorded and placed in an Eppendorf tube containing 800 µl of a reaction mixture comprising of 10 mM H_2O_2, 10 mM KCN, 80 µM NBT and 78.75 mM KPO_4. This was followed by incubating at room temperature for 20 minutes, whereafter the leaf discs and roots were ground in their respective tubes. The plant material was pelleted by centrifuging for 5 minutes at 13000 x g. An aliquot of 200 µl was used to measure the absorbance at 560 nm and O_2 levels was calculated using the extinction coefficient of 12.8 mM^{-1} cm^{-1}.

The spectrophotometric quantification of H_2O_2 was done according to Baptista *et al* (2007), however a few amendments were made. The standards were prepared (0 µM, 5 µM, 10 µM, 15 µM, 20 µM, 25 µM) by diluting a suitable amount of H_2O_2 in distilled water. These samples were added to a microtiter plate in triplicate. The samples were subsequently prepared by mixing 100 mg of the frozen plant material with 500 µl of 6% TCA. Thereafter, 50 µl of the TCA extracts were added to the microtiter plate in triplicate. This was followed by the addition of 1.25 mM K_2HPO_4 and 250 mM KI to each sample and standard in the microtiter plate. The plate containing all the solutions was incubated at room temperature for 20 minutes, with shaking. The absorbance was ultimately measured at 390 nm.

2.8. Estimation of cell death

The estimation of cell death was determined by means of a spectrophotometric assay aimed at measuring the amount of Evans blue retained by non-viable cells (Sanevas *et al*., 2007). For measurement in the leaves, 1 cm^3 blocks were cut from the leaf edge and from the roots, 2 cm fragments were cut from the root tip. The material mass was then

recorded, followed by placing it into Eppendorf tubes containing 1 ml of 0.25% Evans blue and incubated at room temperature for 1 hour. To wash off all the unbound dye, the leaf and root material was incubated in deionized water overnight at room temperature. The water was subsequently discarded and the material was placed in 1% (w/v) aqueous SDS and incubated at 65°C to release all the trapped Evans blue from the cells. An aliquot of 200 μl of the supernatant was used to spectrophotometrically determine the optical density at 600 nm.

2.9. Determination of chlorophyll A and B

The determination of chlorophyll content was done according to Velcheva *et al* (2012), with a few amendments made. For each sample, 100 mg of leaf material was placed into separate Eppendorf tubes. Thereafter, 1 ml of 100% acetone was added, followed by vigorous mixing. The mixtures were subsequently transferred to separate McCartney bottles each containing 9 ml of acetone. The solutions were filtered through Whatman filter paper, and from the purified solution, 2 ml of each sample was placed into separate quartz cuvettes before subsequent spectrophotometric analysis at wavelengths 662 and 644 nm.

2.10. Spectrophotometric quantification of zirconium

The quantification of Zr was done according to Mohammed and Ahmad (2009), however, a few modifications were made for this study. For each sample, 100 mg of leaf material was digested with 500 μl of 65% HNO_3 for 1 hour at 65°C. After incubation, 500 μl of distilled water was added to each digestion mixture, prior to use. Additionally, standards of $ZrCl_4$ (0, 100, 200, 300, and 400 μg/ml) were also prepared. Thereafter, 1

ml of each standard/sample was placed into separate McCartney bottles, to which the following solution was added: 1.6 ml of 4 M HNO_3, 200 µl of 5% ascorbic acid, 2.2 ml distilled water and 1 ml of 0.1 M trioctylphosphine oxide (TOPO). The mixtures were shaken for 3 minutes, where after 400 µl of the organic phase was collected and transferred to clean containers. To each organic phase, 2 ml of 2 mM eriochrome cyanine R (ECR) and 2 ml of TEA-HCl (pH 6.2) was added. The pH of the mixture was adjusted to pH 6.2 by using the appropriate amount of 0.1 M NaOH and 0.1 M HCl, where-after each solution was incubated at room temperature for 10 minutes. The absorbance was ultimately measured at 500 nm for each sample.

2.11. Quantification of zirconium by ICP-OES

For the quantification of Zr in the leaves and roots of *B. napus* L. genotypes, 150 mg of plant material was digested in 1 ml of 65% HNO_3 for 1 hour at 65ºC. Following incubation, each sample was diluted (1:10, v/v) in 4% HNO_3. The samples were analysed by axially-viewed inductively coupled plasma optical emission spectrometry (ICP-OES, Varian Vista Pro).

2.12. Synthesis of CdTe/ZnS Quantum Dots

The CdTe/ZnS QDs used in this study was synthesized according to previous studies, with slight made (Chomoucka *et al*., 2013; Yan *et al*., 2010). The first step of synthesis involved the preparation of NaHTe by dissolving appropriate amounts of $NaBH_4$ (1 mmol) and Te (0.04 mmol) in 10 ml of deionized water. This solution was heated at 80ºC for 30 minutes, which results in a colour change from clear to purple. For the subsequent synthesis of CdTe, 5 ml of the NaHTe solution was used. Another solution was prepared

containing 0.4 mmol $CdCl_2$ and 0.6 mmol MPA dissolved in 15 ml of deionized water at pH 11.7, forming the Cd/MPA precursor. This solution was heated to 100°C under inert atmospheric conditions; however, prior to reaching the final temperature, the NaHTe solution was injected at 80°C. The reaction was maintained at 100°C for 2 hours allowing the growth of CdTe nanocrystals. The solution was then rapidly cooled down on ice and added to a mixed zinc and sulphur precursor solution which was prepared by adding zinc acetate (0.1 M) and thiourea (0.1 M) in a final volume of 15 ml of deionized water (pH11.5). Following the mixture of the solutions, it was degassed and subsequently heated to 90°C for 1 hour which allowed the growth of MPA-capped CdTe/ZnS QDs. The solution ultimately changes colour from purple to yellow. The QDs were subsequently stored in a powder form by adding 100% ethanol, followed by centrifugation (Emamdoust *et al*., 2013). The resultant pellet was retained and dried at 54°C to generate a yellow powder.
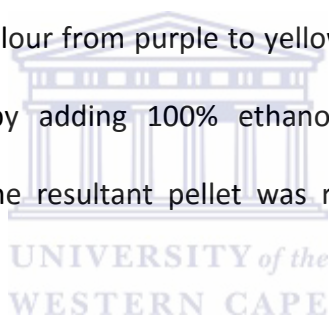
2.13. Preparation of QD/Zr conjugate and subsequent treatment of *B. napus*

The conjugation between CdTe/ZnS core-shell nanoparticles and Zr was done according to Mattoussi *et al* (2000), with a few adjustment made. Conjugation was carried out in a 5 mM sodium borate buffer at pH 9.0. An equal amount of Zr and QD powder was mixed in the buffer for 10 minutes, which subsequently yielded self-assembled QD/Zr conjugates. The resulting solution was stored at room temperature, in the absence of light.

Subsequent treatment of the plants was carried out as described previously, but the treatment solutions were changed; using both conjugated and unconjugated QDs. Each

solution of conjugated QDs used to treat the plants contained 1 mM Zr and 0.233 mg/ml of QDs. The treatment solution of unconjugated QDs only contained 0.233 mg/ml of the nanoparticles.

2.14. Characterization of CdTe/ZnS QDs

Initial analysis of both conjugated and unconjugated QDs were performed using photoluminescence (PL) spectroscopy. PL emission spectra were measured at room temperature using Fluorolog, HORIBA Jobin Yvon. Subsequently, transmission electron microscopy studies were performed using the Hitachi H800, operated at 200 kV.

2.15. *In vivo* imaging of QDs within *B. napus*

Bioimaging of QDs within the plants was done by using the IVIS® Lumina II imaging system and the Living Image software version 3.0 (Caliper Life Science). Two filter sets were used and the results were subsequently overlayed by the system software to generate the images. The GFP filter set included an emission filter (515-575 nm), excitation filter (445-490 nm) and a background filter (410-440 nm). Similarly, the dsRed filter set also included an emission filter (500-550 nm), excitation filter (500-650 nm) and a background filter (460-490 nm). The acquisition of the images was performed with the following system parameters: subject height 0.5 cm, field of view 12.5 cm, lamp level high and an automatic exposure time (0.5-60 seconds).

Chapter 3

Physiological and Biochemical effects of Zirconium on *B. napus* L genotypes
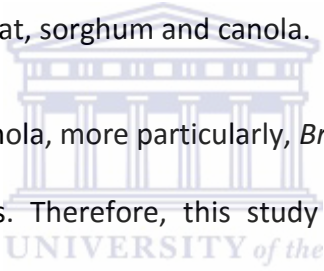
3.1. Introduction

Abiotic stress is currently of great concern globally as it is responsible for the loss of more than 50% of crop yield (Wang *et al*., 2003). These stresses result in the deterioration of the environment and include conditions such as salinity, drought, extreme temperatures, chemical toxicity and heavy metal toxicity. The growth and productivity of plants is negatively affected when they experience stress and subsequently undergo a number of morphological, biochemical, physiological and molecular changes (Wang *et al*., 2003). As a consequence of the sessile nature of plants, they are continuously exposed to these environmental conditions, and have therefore evolved a diverse set of protective mechanisms (Ciarmiello *et al*., 2011; Vickers *et al*., 2009). Depending on the type of stress, plants are able to respond instantaneously to changes in the environmental conditions (Ciarmiello *et al*., 2011). Under abiotic stress, plants prompt for suitable responses, by altering their metabolism, growth and development. They achieve this by various regulatory mechanisms such as stress sensors, signalling pathways consisting of a number of protein-protein interactions, transcription factors and promoters and ultimately the production of specific proteins or metabolites (Ciarmiello *et al*., 2011). One of the most important pathways involved in alleviating stress in plants is the antioxidant-ROS pathway. Studies have shown that

when plants experience stress conditions they overproduce various toxic molecules known as ROS, via the antioxidant pathway; which includes H_2O_2, O_2^-, $OH\bullet$ and $^1O_2$ (Shao *et al.*, 2008; Fodor *et al.*, 2005). Plants have however evolved and developed the ability to respond to these molecules by way of antioxidative mechanisms; these include antioxidants such as ascorbic acid and glutathione, as well as genes such as SOD (scavenges O_2^-), CAT (scavenges H_2O_2) and APX (scavenges H_2O_2). These responses are however not singular processes, but involve a network of pathways, which together with other cofactors and signalling molecules help the plant regulate particular responses to environmental stimuli (Dombrowski, 2003).

In South Africa, extreme environmental changes such as periodic drought stages, increased mining activity (leading to increased HM concentrations in soils), and high soil salinity all have negative effects on plants and ultimately results in poor crop quality (Yadav, 2010). As a consequence of the constant reduction in arable land that South Africa faces, with only 13.5% of the land being suitable for crop production, it is important to make inroads in understanding the pathways that lead to the death of plant cells and senescence (Mohamed, 2000). This reduction of appropriate land for sustainable crop production has subsequently led to an increased demand for food supply and has become a huge problem in South Africa, as studies show that the population increases by 1.5% each year (Statistics South Africa, 2011). This issue therefore requires South Africa to use the arable land optimally. However, 6% of this land is currently utilized for mining, urban and industrial development, which further contributes to the reduction in arable land available (Palmer and Ainslie, 2005). South Africa has become one of the chief producers of a wide selection of minerals (e.g. gold,

vanadium, zirconium, antimony etc.), not only in Africa, but worldwide. It is estimated that mineral sales have reached about R23-trillion thus far and it also constitutes the world's largest reserves of gold, chrome, manganese and the second-largest reserves of vanadium and zirconium. South Africa and Australia produce 80% of the world's zirconium (Emsley, 2001). The mining industry is therefore one of the main driving forces behind the South African economy. However, studies have shown that metals like vanadium and antimony at high concentrations in soils lead to a drastic decline in plant growth (Fenga *et al*., 2013; Feng *et al*., 2009; Xuan Tham *et al*., 2001). Research in this field is thus essential for sustaining optimal production of some of the most important crops like maize, soybean, wheat, sorghum and canola.

No studies have focused on canola, more particularly, *Brassica napus* L and its response to Zr-induced oxidative stress. Therefore, this study investigated the effect of Zr treatment on two genotypes of *B. napus* L.; Agamax and Garnet. It will aim to determine the differential responses of these genotypes to Zr stress. Various factors will be investigated to determine how these plants are affected when exposed to Zr and what measures they implement in order to survive under oxidative stress.

3.3.   Results

3.2.1. Plant growth parameters

In order to assess the effect of treatment with Zr on the two genotypes of *Brassica napus* L, the leaves of the Zr treated and untreated control plants were compared. The growth parameters of both genotypes appeared to be negatively affected by treatment with Zr. Although the Agamax genotype shows no significant changes in its leaf morphology

(Figure 1 A), a significant reduction in the leaf biomass of the treated plants was observed; displaying a ± 47% decrease when compared to the control (Figure 4 A). Similarly, the roots of Agamax showed a decrease in its biomass by approximately 42% (Firgure 2 & 4 B). In contrast, the Garnet genotype displayed substantial changes in leaf morphology between the Zr treated and untreated control plants in terms of leaf area, shape, vein pattern, thickness and texture (Figure 1 B). Furthermore, Zr-treated Garnet plants displayed a decrease in biomass by approximately 77% (Figure 4 A). Root biomass in Garnet plants displayed a similar trend following Zr treatment, revealing a ± 62% decrease (Figure 3 and 4 B).
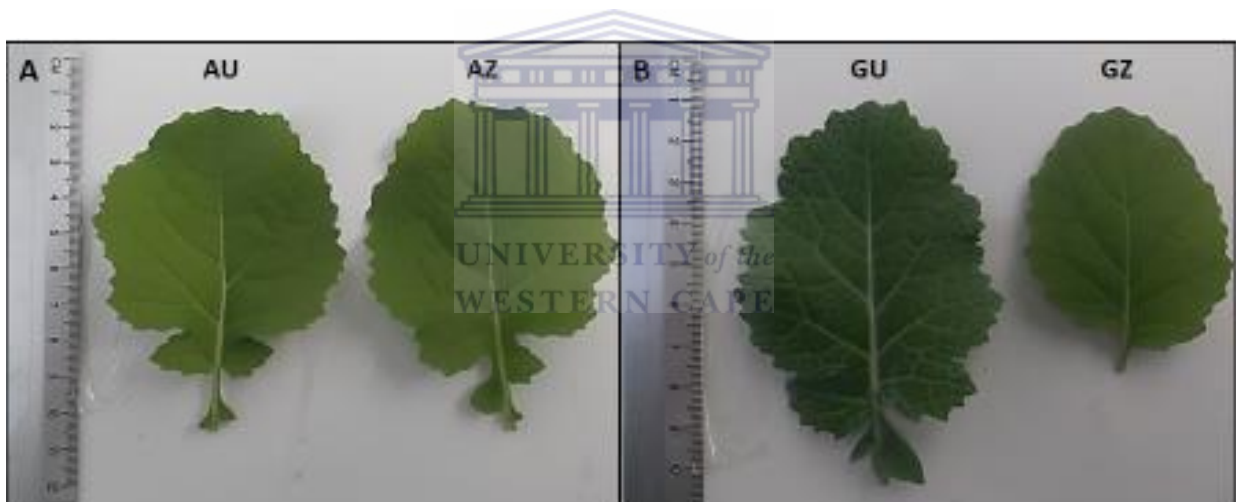
Figure 1: Effect of zirconium on leaf morphology of *Brassica napus* L. The leaves were collected after 28 days, following treatment with Zr (AZ and GZ) or water (AU and GU). The two genotypes, Agamax (A) and Garnet (B) were subsequently analysed by observing their respective morphological differences.

Figure 2: Effect of zirconium on roots of Agamax. Analysis was done by comparing the root length between the untreated (AU) and Zr-treated (AZ) plants.

Figure 3: Effect of zirconium on root length in Garnet. Analysis was done by comparing the root length between the untreated (GU) and Zr-treated (GZ) plants.
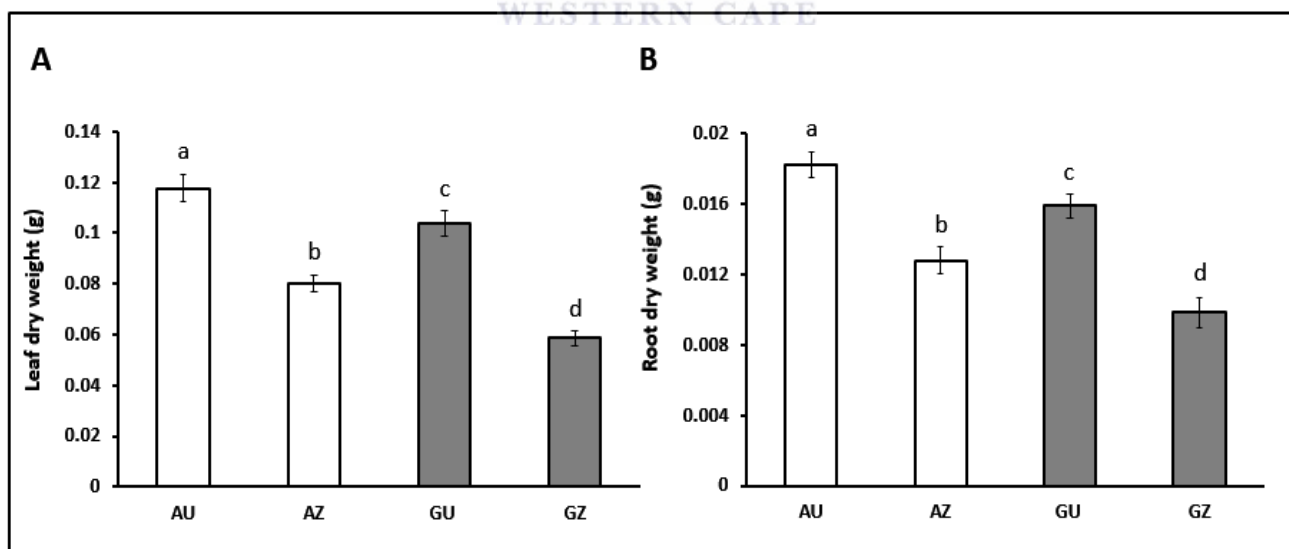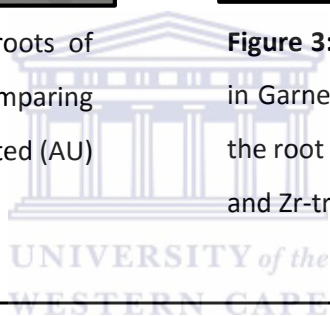
Figure 4: Effect of zirconium on plant biomass. Plants were analysed after 28 days of treatment. (A) Displays the effect of Zr on the leaf dry weights (biomass). (B) Exhibits the root biomass after being treated with Zr. Data represents the mean (±SE) of two independent experiments from six plants per treatment in each experiment. Means with different letters are significantly different from each other ($p < 0.05$).

3.2.2. Cell Death

It has been shown that heavy metals induce oxidative stress in higher plants, which subsequently results in the increased generation of ROS (Zhang *et al.*, 2007). These molecules rapidly destroy biomolecules such as nucleic acids, proteins and lipids, thus leading to cell death. Therefore, following the last treatment of both genotypes, the cell death was measured by means of Evans blue uptake in the leaves and roots. It was generally observed that both genotypes experienced a loss in cell viability in both leaves and roots when treated with Zr (Figure 5 A and B). The level of cell death in the leaves and roots of Zr treated Garnet plants were higher than that of its respective controls (displaying increases of ± 45% and ± 66% in the leaves and roots respectively). The degree of cell death in Agamax treated plants was significantly less than that observed in the Garnet genotype; exhibiting increases of ± 22% in the leaves and ± 33% in the roots, when compared to the control.
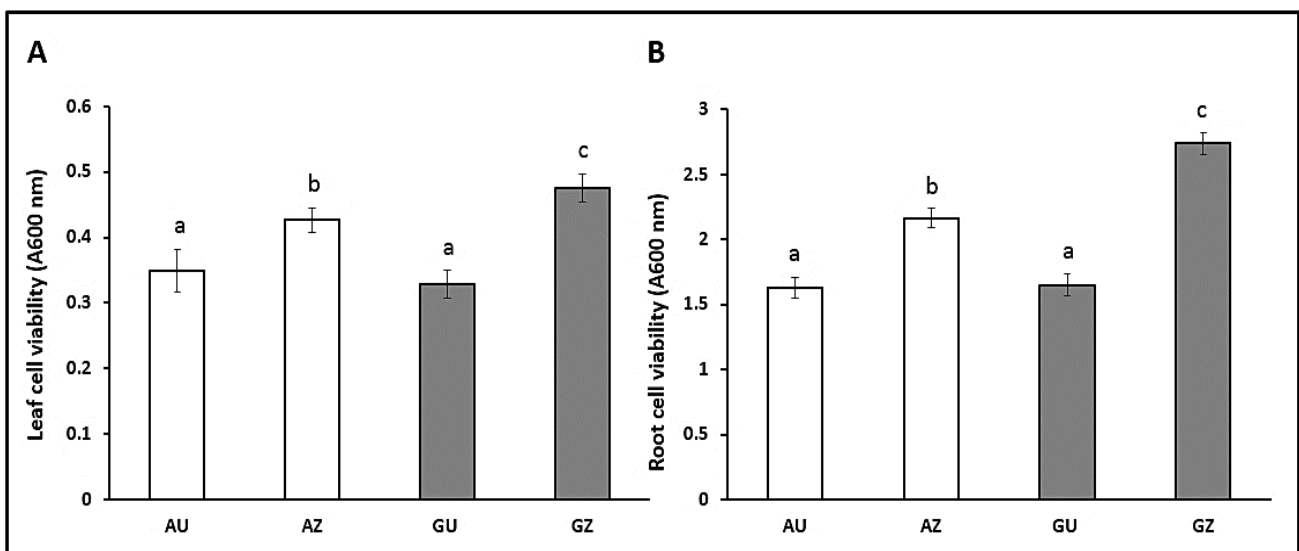
Figure 5: Effect of zirconium on plant cell viability. Plants were analysed after 28 days of treatment. (A) Displays the effect of Zr on cell viability in the leaves. (B) Exhibits the level of cell death due to treatment with Zr in the roots. Data represents the mean (±SE) of two independent experiments from six plants per treatment in each experiment. Means with different letters are significantly different from each other (p < 0.05).

35

3.2.3. Chlorophyll content

It has been shown that plants treated with heavy metals experience a loss of green colour in the leaves, and this is said to be as a result of a decrease in the photosynthetic rate and consequently chlorophyll content (Fatoba and Emem, 2008; Pahlsson, 1989). Therefore, the chlorophyll content of the untreated control plants and the Zr treated plants were measured and compared. The chlorophyll a and b content in the Agamax control and Zr treated plants was observed to be unaffected as their relative quantities were statistically similar when compared (Table 1). The same trendwas observed for the total chlorophyll content, where the amount between the two differently treated Agamax plants are statistically the same. Contrastingly, the chlorophyll a and b content in the Zr treated Garnet plants was observed to have experienced a ± 16% and ± 17% decrease respectively, when compared to the untreated control plants. Similarly, a decrease in total chlorophyll content was observed in the Zr treated Garnet plants when compared to the control plants; showing an ± 18% decrease.

Table 1: Changes in chlorophyll a and b ($\mu g.g^{-1}$) in response to treatment with zirconium.

	Chlorophyll a	Chlorophyll b	Total chlorophyll
AU	0.438 ± 0.004^a	0.166 ± 0.002^b	0.603 ± 0.002^c
AZr	0.443 ± 0.003^a	0.159 ± 0.003^b	0.602 ± 0.006^c
GU	0.438 ± 0.005^a	0.161 ± 0.007^b	0.608 ± 0.012^c
GZr	0.368 ± 0.001^d	0.133 ± 0.001^e	0.501 ± 0.001^f

Different letters indicate significant difference between means at $P<0.05$ (DMRT).
Values are means ±SE (n=4).

3.2.4. Lipid peroxidation

The extent of lipid peroxidation has been shown to be closely related to the effects of heavy metals on plants (Wahsha *et al.*, 2012). Therefore, the lipid peroxidation was measured in both genotypes by measuring the MDA content, which is essentially a product of lipid peroxidation. Following treatment with Zr, Agamax displayed an increase of ± 23% and ± 30% in MDA content in the leaves and roots respectively (Figure 6 A and B). Similarly, the leaves and roots of Zr treated Garnet plants also experienced an increase in lipid peroxidation. However, the increase in MDA content within Garnet plants is approximately 2-fold more than that in Agamax leaves and roots; exhibiting increases of ± 59% and ± 60% respectively.
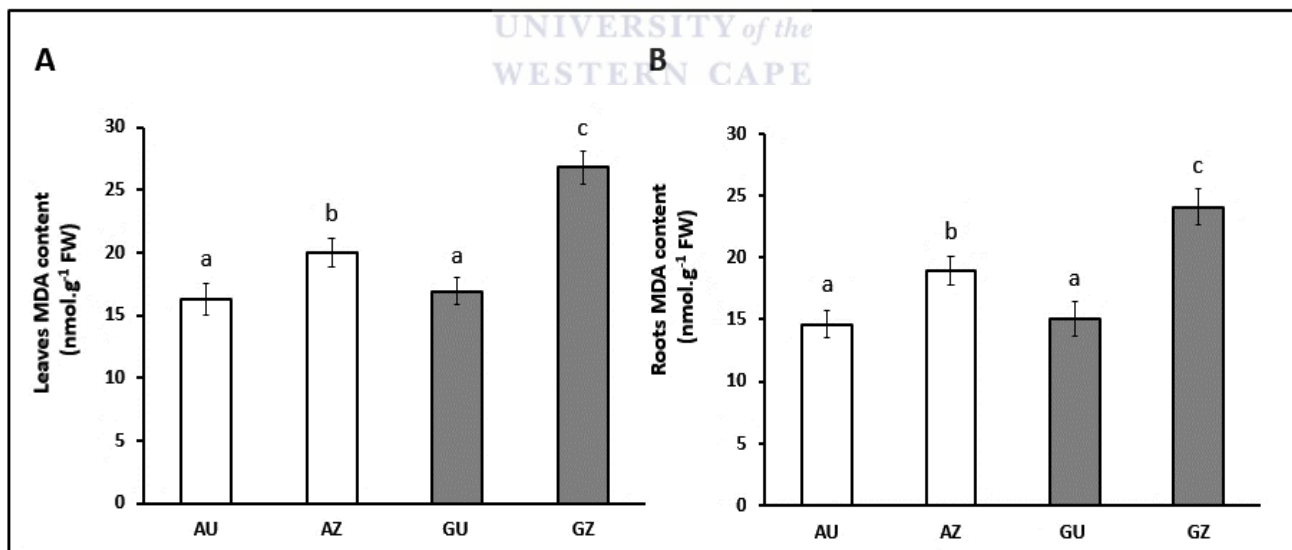
Figure 6: The extent of lipid peroxidation as a consequence of treatment with zirconium in the leaves (A) and roots (B) of *B. napus* L. The MDA content was measured for the analysis Data represents the mean (±SE) of four plants per treatment. Means with different letters are significantly different from each other (p < 0.05).

3.2.5. ROS quantification

Studies have shown that soils containing high concentrations of heavy metals lead to plants experiencing oxidative stress, which consequently leads to the increased production of ROS molecules (Verma and Dubey, 2003). Therefore, the quantification of ROS molecules was performed by measuring O_2^- and H_2O_2. The O_2^- content of Agamax increased by a respective $\pm$ 52% and $\pm$ 53% in the leaves and roots of the Zr treated plants compared to the control plants (Figure 8 A and B). Similarly, a respective increase of $\pm$ 78% and $\pm$ 151% was observed in the leaves and roots of Zr treated Garnet plants. Interestingly, a similar the same trend was observed with regards to H_2O_2 content in the leaves and roots of both genotypes (Figure 7 A and B). Agamax displayed an increase of $\pm$ 26% and $\pm$ 117% in H_2O_2 content, in both leaves ($\pm$ 45%) and roots ($\pm$ 130%).
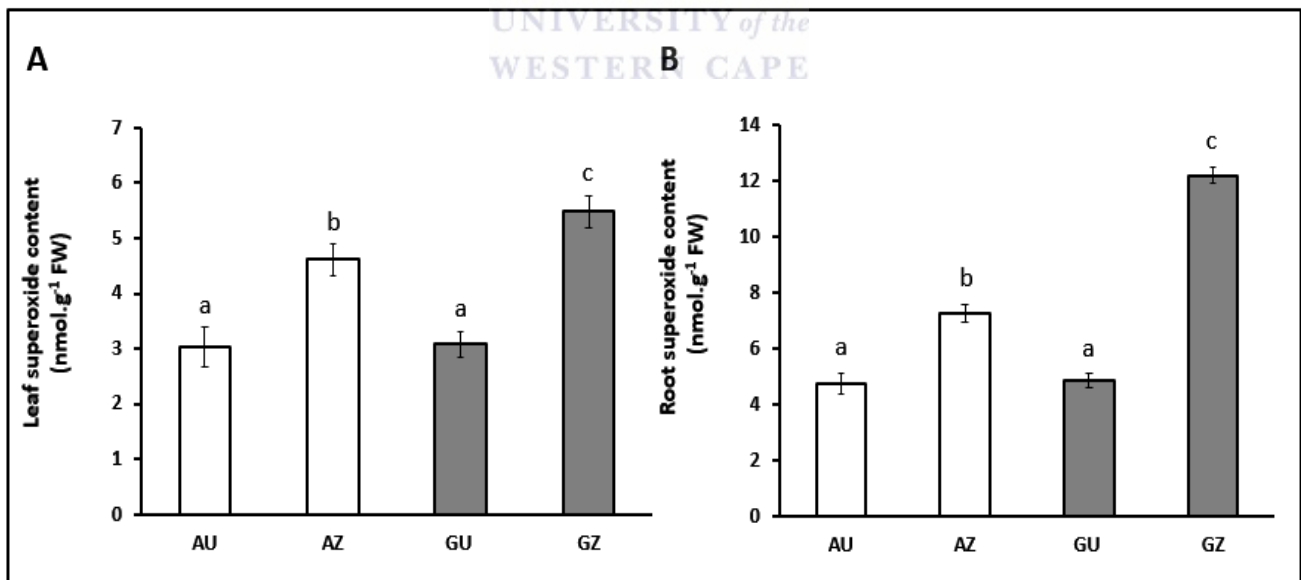
Figure 7: Changes in O_2^- content in response to treatment with zirconium. (A) Displays the effect of Zr-induced oxidative stress on O_2^- content in the leaves. (B) Exhibits the difference in O_2^- content as a result of treatment by Zr in the roots. Data represents the mean ($\pm$SE) of two independent experiments from four plants per treatment in each experiment. Means with different letters are significantly different from each other ($p < 0.05$).
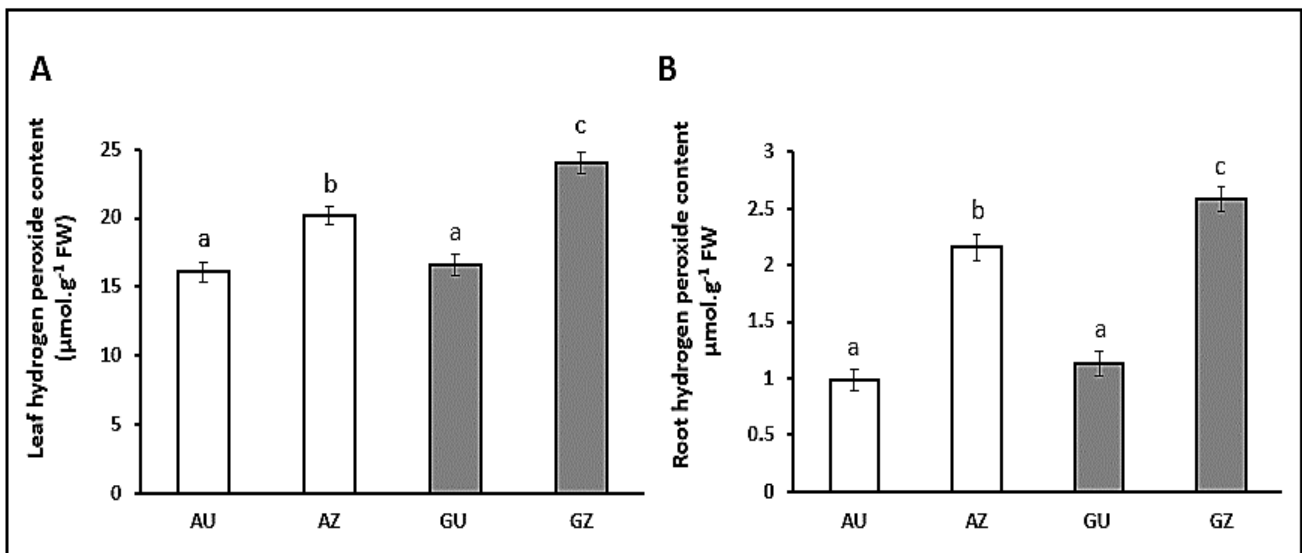
Figure 8: Changes in H_2O_2 content in response to treatment with zirconium. (A) Displays the effect of Zr-induced oxidative stress on H_2O_2 content in the leaves. (B) Exhibits the difference in H_2O_2 content as a result of treatment by Zr in the roots. Data represents the mean (±SE) of two independent experiments from four plants per treatment in each experiment. Means with different letters are significantly different from each other ($p < 0.05$).

3.2.6. Quantification of zirconium in plants

Heavy metals are shown to be taken up in various structures of the plants (Tani and Barrington, 2005). This is said to be indicative of how efficiently plants respond to the toxic effects of heavy metals (Roosens *et al*., 2003). An existing assay was therefore modified to quantify the levels of Zr within various plant structures; which include the leaves and the roots.

When compared to the control plants, Zr treated Agamax leaves displayed a ± 22% increase in concentration of Zr (Figure 9 A). The concentration of Zr in the leaves of Garnet also increased, however much more drastically than in Agamax; increasing by more than ± 120%. The trend in the roots remained the same with both Agamax and Garnet experiencing increases in Zr content when compared to the controls; increasing by ± 32% and ± 59% respectively (Figure 9 B).
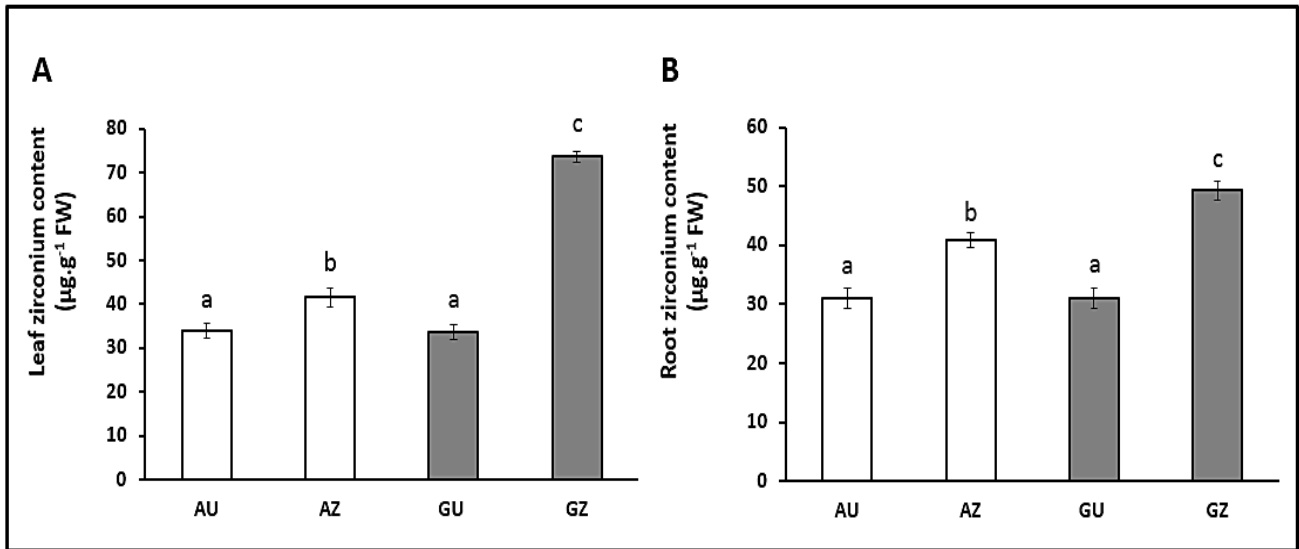
Figure 9: Zirconium concentration in leaves (A) and roots (B) of *B. napus* L genotypes. Data represents the mean (±SE) of four plants per treatment. Means with different letters are significantly different from each other (p < 0.05).

3.2.7. Antioxidant isoform detection

SOD isoform detection revealed a total of six and seven SOD isoenzymes for Garnet and Agamax respectively (Figure 10). The most noticeable difference between the two genotypes of *B. napus* L. is the appearance of an extra SOD isoform in Agamax. The subsequent identification of SOD isoforms was done by Gokul (2013). The subsequent classification of these SOD bands was done according to their metal co-factor, based on their inhibitory pattern. Copper/zinc (Cu/Zn) SODs is inhibited by KCN, H_2O_2 inhibits Cu/Zn SODs and iron (Fe) SODs, and SDS inhibits Mn SODs and iron (Fe) SODs (Brou *et al*., 2007; Cohu and Pilon, 2007; Alscher *et al*., 2002). Essentially, the SOD profile for Agamax included two Mn SODs, two Cu/Zn SODs and three Fe SODs. Garnet's SOD profile was identical to that of Agamax, except for the extra Mn SOD isoform observed in Agamax. Densitometry analysis was used to analyse the relative band intensities and thus measure the relative change in isoform activity to treatment with Zr. In Agamax, no change in activity was observed for Mn SOD 1, Mn SOD 2 and Cu/Zn 2, when compared

40

to their respective controls (Table 2). However, in Garnet, Mn SOD 2 and Cu/Zn SOD 1 showed ± 12% increase and ± 9% decrease respectively, when compared to the controls. No change in activity was observed for Cu/Zn SOD 2 in Garnet. In Agamax, Fe SOD 1, Fe SOD 2 and Fe SOD 3 was shown to increase by ± 24%, ± 13% and ± 28% respectively. However, in Garnet, only Fe SOD 1 exhibited an increase in activity by ± 19%, when compared to the control. Fe SOD 2 and Fe SOD, contrastingly displayed no change in activity.

APX isoform detection showed the presence of seven APX isoforms in both Agamax and Garnet (Figure 11). Isoform activity was subsequently measured by densitometry analysis (Table 3). When compared to their respective controls, APX isoforms 1, 2, 3, 6 and 7 in Agamax displayed no change in activity. Contrastingly, in Garnet, APX isoforms 1, 2, 3 and 7 exhibited increases in activity by ± 24%, ± 37%, ± 36% and ± 9% respectively. However, APX 6 in Garnet displayed no significant change in its activity when compared to the control. APX isoforms 4 and 5 in Agamax showed a ± 23% and ±19% respectively, when compared the controls. Similarly, these APX isoforms also increased in Garnet, as they displayed a ± 42% and ± 39% increase respectively.
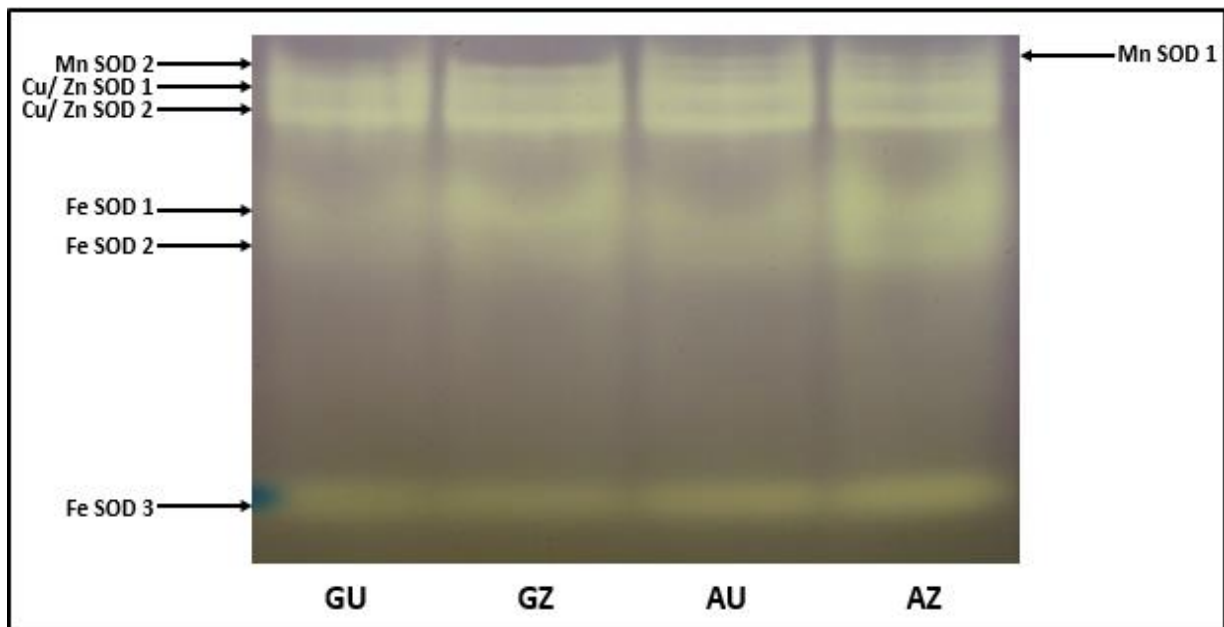
Figure 10: Changes in SOD enzymatic activity in response to treatment with zirconium. Isoform-specific SOD activity was identified using in-gel assays in total soluble protein extracts of the leaves.

Table 2: Densitometry readings for SOD native PAGE activity gel.

Proposed SOD type	GU	GZ	AU	AZ
Mn SOD 1			89 ± 1.26^a	87 ± 1.31^a
Mn SOD 2	96 ± 1.31^c	107 ± 1.25^d	84 ± 1.41^b	82 ± 1.37^b
Cu/Zn SOD 1	99 ± 1.50^f	90 ± 1.33^a	96 ± 1.29^c	84 ± 1.55^b
Cu/Zn SOD 2	82 ± 1.33^b	83 ± 1.39^b	80 ± 1.49^b	84 ± 1.51^b
Fe SOD 1	49 ± 1.57^h	62 ± 1.49^i	49 ± 1.57^h	65 ± 1.52^i
Fe SOD 2	29 ± 1.27^j	34 ± 1.35^k	35 ± 1.41^k	40 ± 1.29^l
Fe SOD 3	25 ± 1.57^m	25 ± 1.49^m	26 ± 1.54^m	36 ± 1.56^k

Different letters indicate significant difference between means at $P<0.05$ (DMRT).

Values are means ±SE (n=4).
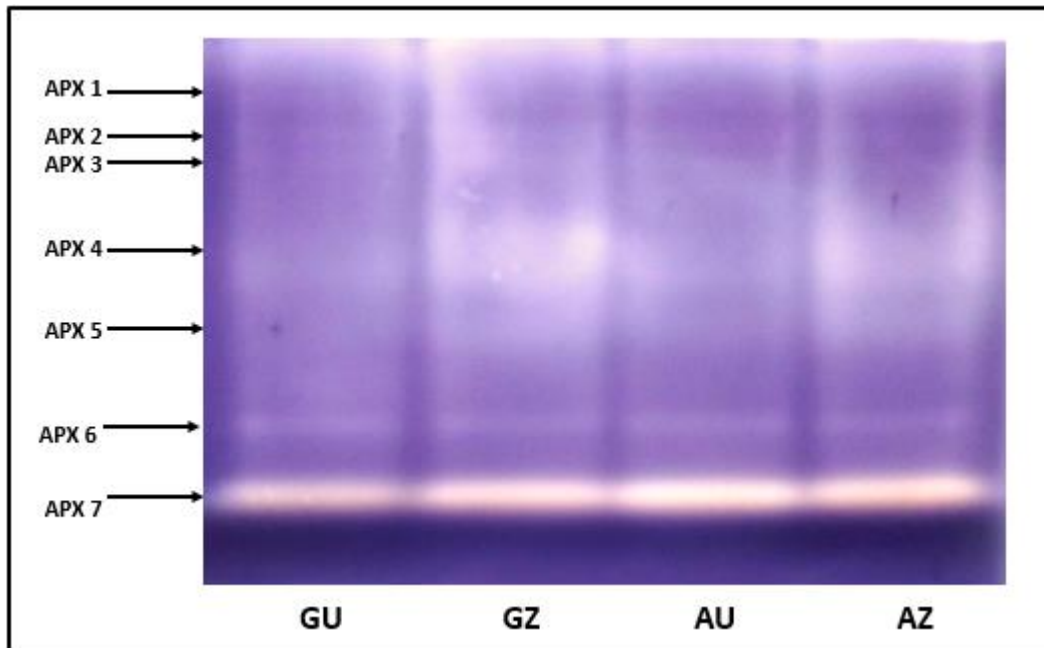
Figure 11: Changes in APX enzymatic activity in response to treatment with zirconium. APX isoform activity was detected using in-gel assays in total soluble protein extracts of the leaves.

Table 3: Densitometry readings for APX native PAGE activity.

	GU	GZ	AU	AZ
APX 1	41 ± 1.56[a]	54 ± 1.69[b]	23 ± 1.54[c]	20 ± 1.65[c]
APX 2	56 ± 1.55[b]	89 ± 1.57[d]	54 ± 1.61[b]	52 ± 1.65[b]
APX 3	55 ± 1.65[b]	86 ± 1.63[d]	73 ± 1.60[e]	70 ± 1.66[e]
APX 4	66 ± 1.59[f]	113 ± 1.61[g]	74 ± 1.63[e]	96 ± 1.60[f]
APX 5	43 ± 1.38[a]	70 ± 1.61[e]	39 ± 1.35[a]	48 ± 1.60[h]
APX 6	48 ± 1.55[h]	47 ± 1.63[h]	48 ± 1.52[h]	45 ± 1.46[h]
APX 7	92 ± 1.62[d]	101 ± 1.58[i]	119 ± 1.65[j]	116 ± 1.61[j]

Different letters indicate significant difference between means at P<0.05 (DMRT). Values are means ±SE (n=4).

3.3. Discussion

Previous studies have suggested that the primary method of determining the effect of heavy metals on plants is to assess the germination of the seedlings (Kavuličová *et al.*, 2012; Di Salvatore *et al.*, 2008). It has been found that heavy metals have several negative effects on plants which include delaying germination, decreasing the rate of germination, and inhibiting the growth of the shoots and roots. Therefore, part of this study assessed the effects of different concentrations of Zr on the germination of Agamax and Garnet seedlings (supplementary figure 1). The seedlings of both canola genotypes were found to experience the same negative effects that were previously described; which seemed to be accelerated by an increase in Zr concentration (supplementary table 1). Similar results were obtained when wheat seedlings were subjected to various concentrations of Zr (Fodor *et al.*, 2005). Fodor *et al* (2005) observed that Zr decreased the germination rate and triggered various physiological alterations. However, it has been shown that the defence mechanisms of plants in the seedling stage of growth is not fully developed (Liu *et al.*, 2005). Therefore, in our study the plants were grown to a more mature growth stage, where further analysis was done to understand responses to Zr stress.

After treatment of the plants with Zr, the biomass was determined. It was subsequently found that the leaf and root biomass of both *B. napus* L. genotypes treated with Zr decreased, however, more so in Garnet (Figure 4). The phenotypical decrease in leaf area was visibly noticeable in Garnet leaves (Figure 1 B), whereas the leaves among Agamax plants appeared relatively similar in size (Figure 1 A). Several authors have also noted that plants exposed to heavy metals experience a decrease in biomass (Kavuličová

44

et al., 2012; Ozturk *et al.,* 2010; Cao *et al.,* 2009). More specifically, Schützendübel and Polle (2002) showed that cadmium (Cd) concentrations higher than 15 µM caused an approximate decrease of 35% in the leaf biomass of pine seedlings. A decrease in biomass was also seen in the leaves and roots of water hyacinths as a result of lead toxicity at 1000 mg/L (Malar *et al.,* 2014). It was noted that the leaves experienced a greater effect of this toxicity, which was thought to be caused by the translocation and accumulation of lead in the leaves.

Heavy metals are said to cause oxidative stress in plants by means of inducing the overproduction of ROS molecules (Verma and Dubey, 2003). One of the downstream effects of excess ROS includes lipid peroxidation, which is believed to be a good indicator of free radical production and tissue damage (Zhang *et al.,* 2007). In our study, it was found that the levels of MDA increased in the leaves of both genotypes of *B. napus* L. that were exposed to Zr (Figure 6). However, a distinguishable difference in these levels were seen between the canola genotypes; with Garnet producing higher levels of MDA in both the leaves and roots, thus indicating a higher degree of lipid peroxidation. This coincides with the trend observed by Zhang *et al* (2007), which showed that heavy metal concentrations outside the tolerance threshold of two mangrove species caused an increase in MDA levels in the leaves and roots. Similarly, Wahsha *et al* (2012) showed an increase in MDA levels in both leaves and roots of *Taraxacum officinale* (dandelion), which grew in an abandoned mine area. It is suggested that heavy metals are absorbed through the roots of the plant and could thus increase lipid peroxidation through excessive free radical generation. The increase in MDA concentration due to the overproduction of ROS could subsequently lead to cell death.

In our study, it was shown that both Agamax and Garnet experienced a certain degree of cell death in both leaves and roots when treated with Zr (Figure 5). The extent of cell death in Garnet was however significantly higher than that observed in Agamax, and thus could explain their individual physiological responses to treatment with Zr. Similar results were observed by Chang *et al* (2005), where they showed that (Zinc) Zn induced cell death in the roots of *Oryza sativa* L. Cell death was first seen at a concentration of 1 mM Zn, and was ultimately noted that this effect increased with an increase in concentration. A study by Schützendübel and Polle (2002) similarly found that (Cadmium) Cd also induces cell death in the leaves of pine seedlings. As a consequence it was proposed that heavy metals are involved in cell wall rigidification, lignification, and DNA fragmentation, thus resulting in cell death (Schützendübel and Polle, 2002).

A study done by Fatoba and Emem (2008) suggests that a good bio-indicator of heavy metal pollution in soils is the chlorophyll content of plants. Therefore, our study measured chlorophyll content in *B. napus* L. genotypes after being exposed to Zr. It was found that only Garnet genotypes treated with Zr experienced a reduction in chlorophyll a and b, as well as a decrease in total chlorophyll content (Table 1). It was similarly shown by Fatoba and Emem (2008) that Cu, Cd, Pb and Fe all caused a decrease in chlorophyll content of *Barbula lambarenensis*. Furthermore, it was observed that an increase in concentration of a particular heavy metal increased the extent of chlorophyll loss. Additionally, Porter and Richard (1981) showed that Zn also caused a decrease in chlorophyll content of vernal alfalfa. A similar study by Fodor *et al* (2005) also found that Zr caused a decrease in chlorophyll content in wheat seedlings. It was suggested that the decrease in chlorophyll content by Zr toxicity in plants could essentially be due to

the temporary inhibition of photosynthesis, increased respiration, reduction in chlorophyll a and b, and the considerable loss of intracellular potassium (Fatoba and Emem, 2008; Pahlsson, 1989).

Heavy metal toxicity is believed to induce the overproduction of ROS molecules, which if not scavenged efficiently by plants, can lead to a decrease in growth rate, chlorosis, lipid peroxidation and ultimately cell death (Kavuličová et al., 2012; Fatoba and Emem, 2008; Zhang et al., 2007). One of the first ROS molecules to be generated is O_2^- (Gill and Tuteja 2010). Following the determination of O_2^- content in both $B.$ $napus$ L. genotypes, it was found that both Agamax and Garnet generated increased amounts of O_2^- in the leaves and roots when compared to the controls (Figure 7). However, the production of O_2^- in Garnet was significantly higher in the leaves and the roots, which could suggest that it experienced a greater degree of oxidative stress under the same conditions. This could be attributed to its inability produce particular enzymes to effectively scavenge O_2^-, such as SOD (discussed later). A similar trend was observed by Li et al (2007) in the leaves of wheat seedlings; as it showed that arsenic (As) was responsible for an increase in O_2^- concentration. This rise in O_2^- concentration was proportional to the concentration of As, where significant increases were observed from 0.5 mg/kg. Another study by Draźkiewicz et al (2004) similarly observed that Cu was responsible for an increase in O_2^- levels in the leaves of $Arabidopsis$ $thaliana$. Ali et al (2006) also showed the increase in O_2^- concentration at 50 µM in the roots of $Panax$ $ginseng$. It was suggested that this could be as a result of a slight decrease in SOD activity. However, In the event of SOD being unable to sufficiently scavenge O_2^- beyond a certain threshold, it would

consequently lead to more significant damages to the cell structures, therefore resulting in a greater degree of cell death.

Another important ROS molecule is H_2O_2, as it has two functions in plants: at low concentrations, it has a role as a signalling molecule to aid in its tolerance to various stresses, and at higher concentrations, it leads to cell death (Quan *et al*., 2008). In our study, it was observed that both Agamax and Garnet experienced an increase in H_2O_2 concentration (Figure 8). Like O_2^-, H_2O_2 levels were also found to be greater in both the leaves and roots of Garnet. Similar increases in H_2O_2 were also observed by Eriyarnremu *et al* (2007), where they showed that Cd and Pb were responsible for an increase in H_2O_2 concentration in the leaves of *Vigna unguiculata*. Another study by Draźkiewicz *et al* (2004) showed that Cu induces oxidative stress in the leaves of *Arabidopsis thaliana*, which subsequently also resulted in an increased generation of H_2O_2 molecules. It was suggested that at particular concentrations of Cu, H_2O_2 levels were elevated as a result of a decrease in APX activity (Draźkiewicz *et al*., 2003). Like O_2^-, H_2O_2 production was also found increase in the roots of *Panax ginseng* at a concentration of 50 μM. Essentially, heavy metal-induced oxidative stress is associated with an increase in the generation of ROS molecules, particularly O_2^- and H_2O_2 in various structures of the plant. As a result, plants naturally induced an increase in antioxidant enzymatic activity to overcome the oxidative stress.

The dismutation of O_2^- molecules in plants is carried out by SOD (Gill and Tuteja, 2010). This is one of the defensive mechanisms plants possess to help detoxify ROS molecules. In our study, a total of 6 and 7 SOD isoforms were identified for Garnet and Agamax

respectively (Figure 10). In Agamax, an increase in activity was observed for three of the Fe SOD isoforms, while the rest of the SOD isoforms exhibited no change in activity when compared to the controls. Contrastingly, in Garnet, only Fe SOD 1 and Mn SOD 2 exhibited an increase in activity, while Cu/Zn SOD 1 was shown to decrease. The rest of the SOD isoforms in Garnet displayed no change in activity when compared to the controls. According to Tsang *et al* (1991), SOD is inducible by particular substrates (such as O_2^-), which essentially induce an increase in the expression of genes encoding SOD enzymes. The increase in SOD activity could therefore be attributed to an increase in O_2. Similarly, it was found that SOD activity increased in *Medicago truncatula* wild type plants in response to treatment with Zn (López-Millán *et al.*, 2005). SOD activity was also shown to increase in *B. napus* L. in response to drought stress, however, a total of 8 isoforms were observed; three isoforms of Mn SOD and five isoforms of Cu/Zn SOD (Abedi and Pakniyat, 2010). It was suggested that a higher degree of SOD activity could be associated with a greater ability to scavenge O_2^-, and thus a greater degree of protection against oxidative stress.

It has been recognised that an excess of H_2O_2 in plant cells leads to oxidative stress (Gill and Tuteja, 2010). APX is thought to be the most essential antioxidative enzyme for scavenging H_2O_2 in higher plants; forming H_2O and monodehydroascorbate (DHA) in the process. In our study, a total of 7 APX isoforms were observed in both Agamax and Garnet (Figure 11). Agamax displayed an increase in activity of only two of its isoforms, whereas six isoforms increased in Garnet. The rest of the isoforms in both Agamax and Garnet displayed no change in activity. An increase in APX activity was also observed in the leaves of rapeseed seedlings in response to Zn treatment. Similarly, APX activity was

observed to increase in the leaves of pigeon pea plants in response to treatment with Ni (nickel) and Zn (Madhava Rao and Sresty, 2000). A similar increase in APX activity was observed by Prasad *et al* (1991) in *B. juncea* due to Zn toxicity. It is suggested that the increase of APX observed in our study could be as a consequence of an increase in H_2O_2; and thus might aid in reducing the concentration of H_2O_2.

Another defensive mechanism possessed by plants is its ability to distribute heavy metals throughout the plant structures (Clemens, 2006). All plants species therefore have a basal level of tolerance to particular heavy metals. In our study, it was found that both genotypes of *B. napus* L. accumulated various amounts of Zr in both the leaves and roots (Figure 9). Garnet displayed a higher level of accumulation of Zr in both leaves and roots (under Zr treatment), when compared to Agamax. It was also observed that Garnet accumulated higher levels of Zr in its leaves, whereas Agamax generally retained Zr in its roots. Similarly, Pickering *et al* (2000) found Ar to be taken up by the roots of *B. juncea*, where a small amount was subsequently transported to the leaves. Marchiol *et al* (2004) also observed that *B. napus* accumulated metals such as Cd, Cr, Cu, Ni, Pb and Zn. The general pattern displayed by *B*. napus was that it accumulated higher concentrations of heavy metals in the roots, than in the leaves; which coincide with the findings seen in Agamax (in our study). These different distribution patterns of Zr throughout the structures of both genotypes could help justify the previously discussed effects on these plants.

Studies have found that particular concentrations of heavy metals may be toxic to plants (Clemens, 2006). Therefore, given that Garnet transports the bulk of its Zr to the leaves,

it could justify why signs of chlorosis was observed in its leaves. Furthermore, the relatively high concentration of Zr in the leaves of Garnet could also account for the higher levels of MDA, cell death and ROS. This could also explain the lower levels of chlorophyll observed in the leaves of Garnet, when compared to Agamax. Additionally, the severe decrease in leaf biomass of Garnet might also be justifiable by the transport of Zr to the leaves. These varying mechanisms of Zr transport between the two genotypes of *B. napus*, together with the differential expression patterns of antioxidant enzymes and difference in SOD enzymatic profiles, may be the determining factors which confer characteristics of tolerance and sensitivity to Zr.

Chapter 4

In vivo imaging of Quantum Dots to trace the uptake of Zirconium in *B. napus* genotypes

4.1. Introduction

Nanotechnology, by definition, is the science of producing machines, devices and systems that apply the unique physical, chemical, optical and biological properties of nanoparticles (Ebbesen and Jensen, 2006). Nanoparticles differ from bulk materials by the fact that their shape and size are able to be manipulated at a nanometer scale. Therefore, nanoparticles have become of great interest because of their targeting and imaging abilities for subsequent use in a range of different areas from biomedical applications to water treatment (Hild *et al.*, 2008). There are several nanoparticles that may be used in targeting applications, and one such particle which is able to perform simultaneous targeting and imaging capabilities is semi-conducting nanoparticles, otherwise known as quantum dots (QDs). These nanoparticles differ from other nanoparticles largely due to their unique optical properties which is a result of the quantum confinement effects of their size and core-shell structure at the nanoscale (Shi *et al.*, 2015).

The use of nanotechnology in agriculture is an emerging field. Although nanoparticles are widely used for biomaging of molecules in animal studies, caution has been show for its use in consumable products (Soenen *et al.*, 2014; Ebbesen and Jensen, 2006). This is mainly due to the great uncertainty of the long-term effects of nanoparticles, which

has subsequently brought about several ethical concerns. Therefore, our study aims to solely use nanoparticles for *in vivo* imaging in plants. The aim of our study was thus to investigate the uptake and translocation of Zr within *B. napus* genotypes by its conjugation to QDs, which would ultimately be imaged using the IVIS Lumina Imaging System. For subsequent quantification of Zr within the plant structures, ICP-OES was used.

4.2. Results

4.2.1. Quantification of zirconium by ICP-OES

Previous studies suggest that plants translocate heavy metals to various structures of the plant (Tani and Barrington, 2005). This mechansim is believed to play a vital role in its survival in areas with high concentrations of heavy metals in the soil. Therefore, the quantification of zirconium in the various plant structures was measured using ICP-OES.

Agamax displayed a ± 40% increase in Zr concentration in the leaves, when compared to the control. In contrast, the leaves of Garnet exhibited a substantially greater increase in Zr when compared to the control; revealing a ± 253% increase. The uptake of Zr in the roots of Agamax and Garnet displayed a completely different trend. Agamax experienced an approximate increase of ± 497%, whereas Garnet displayed a ± 279% in its roots.

Table 1: Quantification of Zr (µg.g^{-1}) in the leaves and roots of *B. napus* genotypes.

	Leaves	Roots
AU	3.24 ± 0.3^a	1.36 ± 0.4 ^{a}
AZr	4.52 ± 0.4^b	677.4 ± 0.3^b
GU	3.02 ± 0.3^a	1.54 ± 0.7 ^{a}
GZr	10.66 ± 0.2^c	431.8 ± 0.6 ^{c}

Different letters indicate significant difference between means at P<0.05 (DMRT). Values are means ±SE (n=4).

4.3.2. Characterization of CdTe/ZnS QDs

The initial characterization of water-soluble CdTe/ZnS semiconducting nanoparticles was done using photoluminescence spectroscopy (Figure 1). The PL spectra of both unconjugated and Zr-conjugated QDs reveal full width half maximums of 144 nm and 134 nm respectively. Both samples were excited at 380 nm, which subsequently yielded emission wavelength of 555 nm and 554 nm respectively. Subsequent analysis of the QDs was carried out by TEM (Figure 2). The image displays monodispersed CdTe/Zn nanoparticles, with some showing a tendency to agglomerate. The particles are spherical in shape and have average diameters ranging from 2-20 nm.
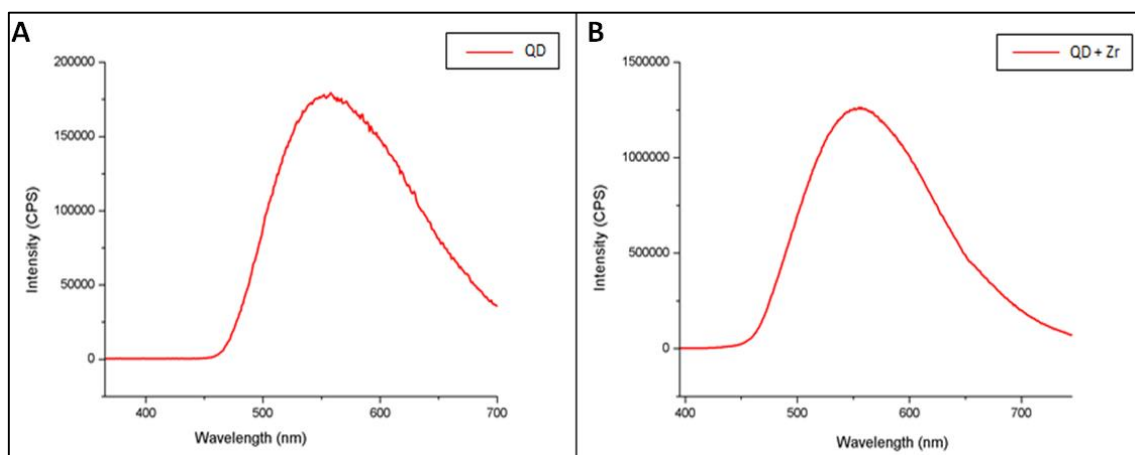
Figure 1: PL spectra of (A) unconjugated and (B) Zr-conjugated CdTe/ZnS quantum dots. Samples were excited at 380 nm, within subsequent PL emission being measured from an optical path length of 5 nm.

Figure 2: TEM micrograph of CdTe/ZnS quantum dots.

4.3.2. *In vivo* imaging of QDs within *B. napus*

In order to see whether the conjugation of Zr to the QDs resulted in a target form of translocation, the unconjugated QDs were used as a positive control. Treatment of both Agamax and Garnet with the unconjugated QDs showed a similar trend in uptake in both the leaves and roots (Figure 3 A and B; Figure 4 A and B). The uptake of these QDs in the roots suggests a widespread form of distribution. However, their relative intensities suggest that Garnet has more nanoparticles emitting light in the roots when compared to Agamax. A similar dispersion pattern was displayed within the leaves of both genotypes, and the intensity of light emitted is relatively the same as well. Contrastingly, when the plants were treated with the conjugated QDs, a complete difference was observed in the translocation and dispersion patterns (Figure 3 C and D; Figure 4 C and D). In the roots of both Agamax and Garnet treated with the conjugated QDs, the same form of distribution is displayed; with the QDs emitting light throughout the length of the root. However, a difference in the intensity of light suggest that Agamax retains a larger portion of the particles within the roots. In contrast, the leaves of both genotypes that were treated with the conjugated QDs reveal a highly targeted form of translocation and distribution; with the QDs emitting light from the periphery of the leaves. The intensity of ligh reveals that Garnet translocates these particles to a greater degree as compared to Agamax.
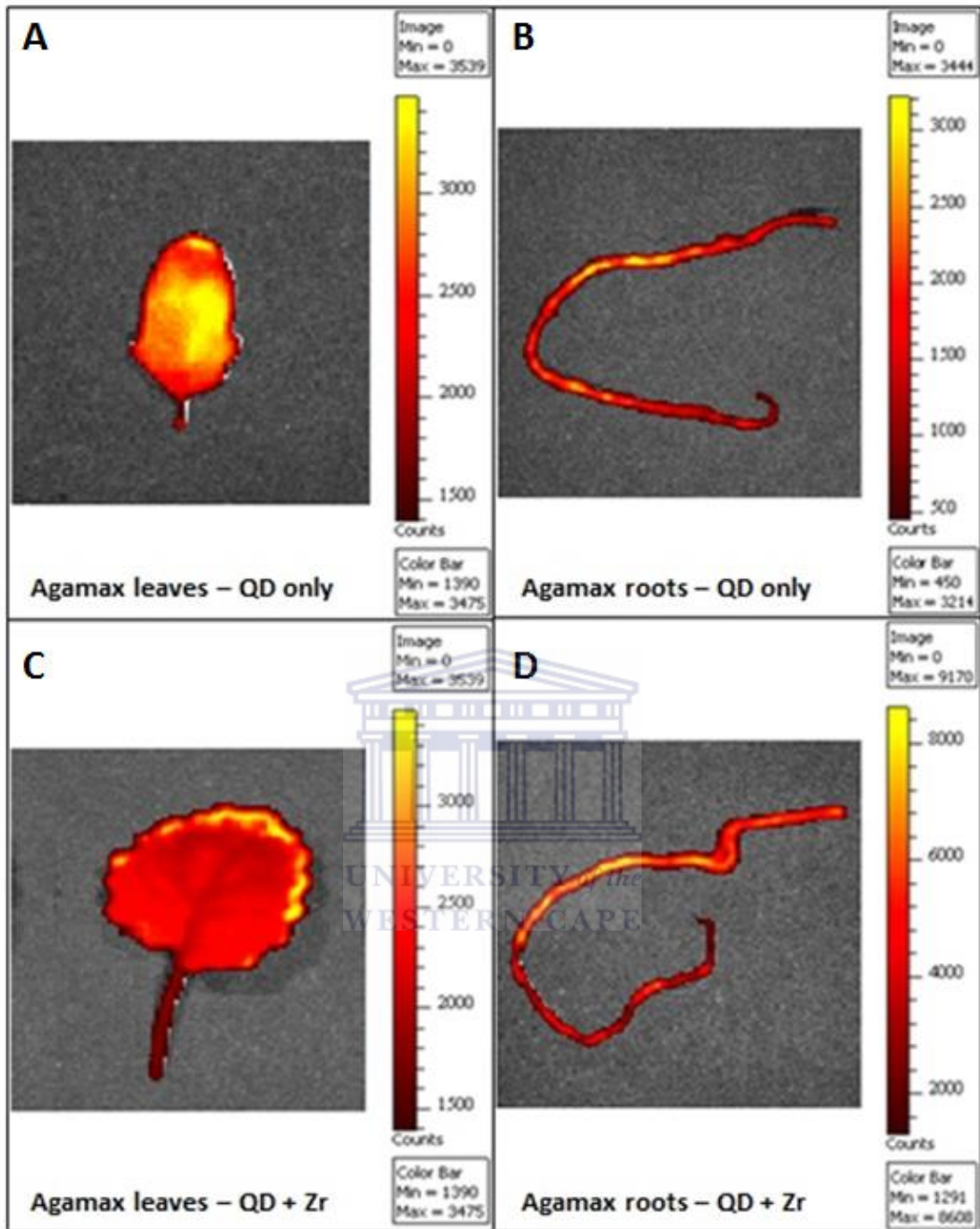
Figure 3: Comparitive uptake of (A & B) unconjugated and (C & D) Zr-conjugated quantum dots within the leaves and roots of Agamax. Colour bars indicate the relative intensity of light emitted. Each image is a representative of a set of 12 images.
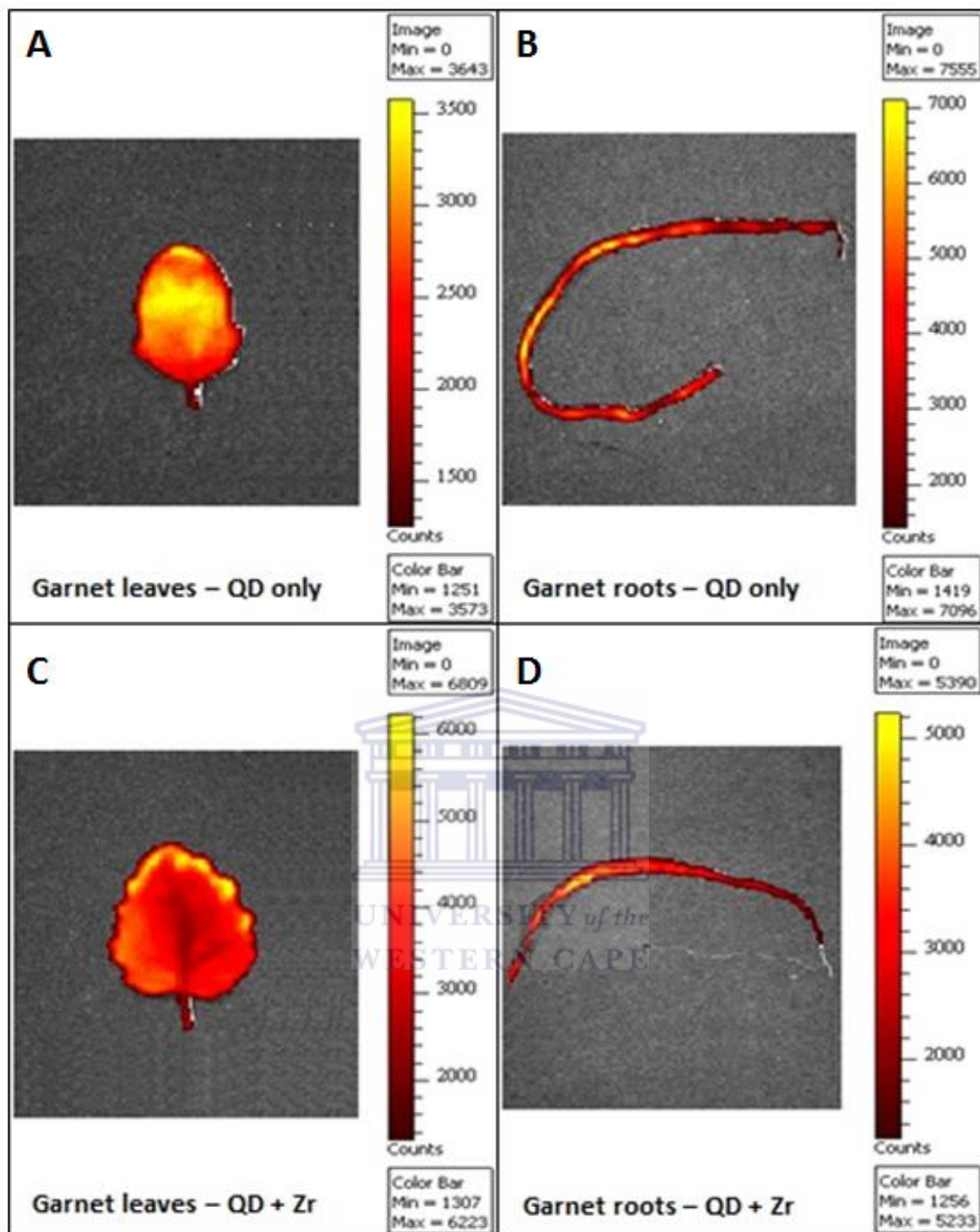
Figure 4: Comparitive uptake of (A & B) unconjugated and (C & D) Zr-conjugated quantum dots within the leaves and roots of Garnet. Colour bars indicate the relative intensity of light emitted. Each image is a representative of a set of 12 images.

4.4. Discussion

It is known that plants naturally possess the ability to tolerate certain levels of heavy metals; one such mechanism allows the distribution of heavy metals throughout the plant structures (Clemens, 2006). As previously described (Chapter 3), both *B. napus* genotypes display accumulation of Zr within their leaves and roots. ICP-OES was subsequently conducted to confirm these reports (Table 1). Similarly, it was found that accumulation of Zr occurred in both genotypes; Garnet displaying greater uptake into the leaves, whereas Agamax largely retained Zr in the roots. A study by Zehra *et al* (2009) showed the accumulation of metals such as Cr, Ni and Cd in *Sylibum marianum*, *Rumex dentatus* and *Cannabis sativa* respectively. Marchiol *et al* (2004) also reveals the uptake of heavy metals such as Pb, Ni, Zn and Cd in *B. napus*; with translocation patterns resembling that of Agamax. For particular metals such as Cr, concentrations of 7.0 ± 0.05 $\mu g.g^{-1}$ was shown in the leaves of *B. napus*; essentially corresponding with concentrations of 4.52 ± 0.4 $\mu g.g^{-1}$ exhibited in the leaves of Agamax. In the same way, Cr levels in the roots corresponded with levels of Zr in Agamax roots; displaying concentrations of 825.0 ± 14.9 $\mu g.g^{-1}$ and 677.4 ± 0.3 $\mu g.g^{-1}$ respectively. As a consequence of the previously described data, our study sought to image the uptake of Zr in *B. napus* by means of QDs.

As aforementioned, water-soluble CdTe/ZnS QDs were synthesised, which essentially contained MPA as the capping ligand. Subsequent conjugation of the QDs was carried out using the principle of electrostatic attraction between the negatively charged mercaptopropionic acid capped core-shell nanoparticles and the positively charged Zr

molecules. The excitation wavelength of these molecules was measured at 380 nm for both the unconjugated and conjugated QDs. The subsequent emission spectrum displayed a PL peak at 555 nm and 554 nm respectively (Figure 1). This data conincided with that described by Yan *et al* (2010); which similarly revealed an emission wavelength for MPA-capped CdTe/ZnS QDs. The QDs fabricated in this study exhibited high fluorescence, in the form of a bright yellow colour. Images provided via TEM show monodispersed QDs, some showing signs of aggregation (Figure 2). A large size distribution is evident through the images, ranging from 2-20 nm. This can be confirmed by the broad FWHM of the PL curves (Duan *et al*., 2009). A study by Shen *et al* (2013) suggests that broad size distribution and relatively small surface/volume ratio of the particles greatly decreases the quantum yield. These factors are controllable by altering the parameters of synthesis such as the reflux time. However, for the purposes of this study, the previously described synthesis of QDs was sufficient for its intended use.

The IVIS Lumina II imaging system is one that is routinely used for non-invasive bioimaging in animal models; usually rodents (Kong *et al*., 2011; Hild *et al*., 2008). However, it proved to be a useful tool for semi-quantitative measurement and spatial distribution of QDs translocation in the leaves and roots of *B. napus* L. genotypes. The filter settings and system software significantly reduced background fluorescence by chlorophyll in the leaves. A study by Zhou *et al* (2005) specifically reported background fluorescence by plant tissues to be problematic when imaging GFP reporters. Other methods of imaging that potentially possess the ability to image QDs within plant tissue, include confocal laser-scanning microscopy and fluorescence microscopy, though analysis may prove to be more qualitative (Stephan *et al*., 2011).

As previously described, ICP-OES data reveals that Agamax retains a large portion of Zr in its roots, whereas Garnet translocate the heavy metal to its leaves. This pattern of uptake and translocation was similarly displayed by images generated by the IVIS Lumina imaging system. An added benefit of this imaging technique was the ability to view the spatial distribution of Zr. This imaging system proved to be successful in tracing the uptake and translocation of QDs within *B. napus*; more importantly allowing visualization of Zr translocation, which was essentially attached to the QDs.

Conclusion and Future Prospectives

This study proved that high concentrations of Zr tend to exhibit detrimental effects on two *B. napus* L cultivars; specifically Garnet and Agamax. These adverse effects have been observed in both cultivars by a delay in germination, decrease in rate of germination percentage and reduction in plant biomass. However, these negative effects appear to be greater in Garnet; suggesting that Agamax is more tolerant to Zr-induced stress. This was supported by a visible decrease in root and leaf biomass in Garnet, whereas in Agamax, no noticeable changes were observed. The leaves of Garnet also showed signs of chlorosis when treated with Zr which was supported by a substantial decrease in chorophyll content, whereas that of Agamax appeared relatively similar to the control. The levels of lipid peroxidation as displayed by the measurement of MDA levels was significantly greater in the leaves and roots of Garnet when compared to Agamax. This was validated by the levels of cell death, which is known to be a consequence of lipid peroxidation. It was found that the levels of cell death were also higher in the leaves and roots of Garnet, when compared to Agamax. An assay to rapidly measure Zr levels in various plant tissues was developed to gain more insight into the uptake of the metal in these *B. napus* L cultivars. It was observed that Garnet acquired large amounts of Zr from the soil through its roots, and subsequently translocated it to the leaves. Similarly, Zr was also taken up from the soil by Agamax, however, only small amounts of Zr was translocated to the leaves. This ability to sequester the bulk of Zr within the roots and prevent its translocation to the leaves comes forth as one of its mechanisms that confer a greater tolerance to Zr-induced stress.

It is well-known that heavy metal toxicity causes oxidative stress in plants, therefore this study evaluated the effect of Zr treatment on the antioxidant scavenging pathway of two *B. napus* L cultivars. To determine the effect of Zr treatment on ROS production, the levels of O_2^- and H_2O_2 were measured. The levels of both O_2^- and H_2O_2 were found to increase in Garnet and Agamax, however, significantly higher levels were found in Garnet. This indicates that Garnet experienced a great degree of oxidative stress when treated with Zr. An increase in ROS is generally associated with the upregulation of scavenging enzymes, therefore the study investigated the effect of Zr-induced oxidative stress on SOD and APX enzymatic activity. The study subsequently identified a total of six SOD isoforms in Garnet; two Mn SODs, two Cu/Zn SODs and three Fe SODs. The SOD profile of Agamax consisted of 7 SOD isoforms which were almost identical to that of Garnet, however, it was comprised on an additional Mn SOD. No significant changes were observed in the expression of these SOD enzymes, but the presence of the extra Mn SOD could attribute to the relatively low levels of O_2^- observed in Agamax. This could be indicative of one of the mechanisms which allow Agamax to exhibit tolerance to Zr. Upon the investigation of APX profiles, it was ultimately revealed that both Garnet and Agamax consisted of a total of seven APX isoforms. Similarly, no noteworthy changes were observed in the expression of APX in both Garnet and Agamax.

This study also revealed the spatial distribution of Zr within the two *B. nappus* L. genotypes, Garnet and Agamax. The images were captured using the IVIS Lumina imaging system and was made possible by conjugating Zr to the surface CdSe/ZnS QDs. The conjugation was based on electrostatic interactions between the negatively charged mercaptopropionic acid capped core-shell nanoparticles and the positively charged Zr

molecules. The images ultimately revealed that Garnet transports the bulk of the Zr from the soil to its leaves, although smaller amounts were observed in its roots. Clear signs of necrosis could be seen on the leaves of Garnet, which was indicative of the site of Zr aggregation within the leaves. Agamax was shown to sequester most of the Zr in its roots, however, smaller amounts were seen in the leaves. These images confirm the findings from the previously described Zr Assay, as well ICP-OES. The IVIS Lumina imaging system was essentially demonstrated to be an ideal tool for the bioimaging of plant tissue. Furthermore, the practical use of nanoparticles such as QDs was perfectly displayed in this study. Its unique physical, chemical and optical properties make them a useful tool for targeting and imaging several other molecules as well.

Future work will entail the use of CdSe/ZnS QDS to trace the uptake of Zr on a cellular level. This imaging will be carried out using confocal microscopy which will reveal the intracellular organelle(s) responsible for the isolation of Zr heavy metals. By altering the size of the QDs, thus changing its emission wavelength, it will ultimately be possible to visualise several other metals simultaneously.

To validate and justify the biochemical results observed in this study, future work will entail a more comprehensive analysis. This will be done by subjecting the antioxidant isoforms of interest to separation by 2D PAGE, where further analysis will be done by software known as PDQuest, which will identify differentially expressed proteins and submit them for further proteomic analysis. This will be carried out by a form of tandem mass spectrometry known as matrix-assisted laser desorption/ionization (MALDI) time-of-flight/time-of-flight (TOF/TOF), which will BLAST the peptide sequence of the isolated proteins and subsequently identify the DNA sequence of the protein by searching

against the Phytozome database. The sequence data will eventually be used for the designing of primers with the aim of amplifying the gene(s) of interest using PCR and subsequent semi-quantitative analysis will be conducted to confirm responses to Zr. The hypothesized enzymatic activity will then be confirmed by expression and purification of the genes, where after it will be inserted into an appropriate plant transformation vector. The resulting construct will ultimately be used to transform other crop plants to determine whether tolerance to Zr can be conveyed using the genes that were identified.

References

Abdul-Wahab SA and Marikar FA (2012) The environmental impact of gold mines: pollution by heavy metals. *Central European Journal of Engineering*, 2(2), pp.304-313.

Abedi T and Pakniyat H (2010) Antioxidant Enzyme Changes in Response to Drought Stress in Ten Cultivars of Oilseed Rape (*Brassica napus* L.). *Czech Journal of Genetics and Plant Breeding*, 46(1), pp.27-34.

Ali MB, Hahn EJ and Paek KY (2006) Copper-induced changes in the growth, oxidative metabolism, and saponin production in suspension culture roots of *Panax ginseng* in bioreactors. *Plant Cell Reports*, 25, pp.1122-1132.

Alivisatos AP, Gu W, and Larabell C (2005) Quantum Dots As Cellular Probes. *Annual Review of Biomedical Engineering*, 7, pp.55-76.

Alscher RG, Erturk N and Heath LS (2002) Role of superoxide dismutases (SODs) in controlling oxidative stress in plants. *Journal of Experimental Botany*, 53(372), pp.1331-1341.

Apel K and Hirt H (2004) Reactive oxygen species: metabolism, oxidative stress, and signal transduction. *Annual review of Plant Biology*, 55, pp.373-399.

Asada K (1994) Production and action of active oxygen species in photosynthetic tissues. In: CH Foyer, PM Mullineaux, eds. Causes of photooxidative stress and amelioration of defense systems in plants. Boca Raton: CRC Press, pp.77-104.

Babbs CF, Pham J and Coolbaugh RC (1989) Lethal Hydroxyl Radical Production in Paraquat-Treated Plants. *Plant Physiology*, 90, pp.1267-1270.

Badawi GH, Yamauchi Y, Shimada E, Sasaki R, Kawano N, Tanaka K and Tanaka K (2004) Enhanced tolerance to salt stress and water deficit by overexpressing superoxide dismutase in tobacco (*Nicotiana tabacum*) chloroplasts. *Plant Sci*ence, 166, pp.919-928.

Bailey-Serres J and Mittler R (2006) The Roles of Reactive Oxygen Species in Plant Cells. *Plant Physiology*, 141(2), p.311.

Baker CJ and Mock NM (1994) An improved method for monitoring cell death in cell suspension and leaf disc assays using Evans blue. *Plant Cell Tissue Organ Culture*, 39, pp.7-12.

Bannister WH, Bannister JV, Barra D, Bond J and Bossa F (1991) Evolutionary Aspects of Superoxide Dismutase: The Copper/Zinc Enzyme. *Free Radical Research*, 12(1), pp.349-361.

Baptista P, Martins A, Salomé Pais M, Tavares RM and Lino-Neto T (2007) Involvement of reactive oxygen species during early stages of ectomycorrhiza establishment between *Castanea sativa* and *Pisolithus tinctorius*. *Mycorrhiza*, 17, pp.85-193.

Barrera G (2012) Ovidative stress and the lipid peroxidation products in cancer progression and therapy. *ISRN Oncology*, 2012, pp.1-21.

Birben E, Murat Sahiner U, Sackesen C, Erzurum S and Kalayci O (2012) Oxidative Stress and Antioxidant Defense. *The World Allergy Organization*, 5(1), pp.9-19.

Blaine S (2012) Census: SA's population of 51.8m is still young. *Business Day*, [online] Available at: < http://www.bdlive.co.za/economy/2012/10/30/census-sas-population-of-51.8m-is-still-young> [Accessed 14 February 2015].

Blokhina O, Virolainen E and Fagerstedt KV (2003) Antioxidants, Oxidative Damage and Oxygen Deprivation Stress: a Review. *Annals of Botany*, 91(2), pp.179-194.

Bowler C, Van Camp W, Van Montagu M, Inzéb D and Asadac K (1994) Superoxide Dismutase in Plants. *Critical Reviews in Plant Sciences*, 13(3), pp.199-218.

Brou YC, Zézé A, Diouf O and Eyletters M (2007) Water stress induces overexpression of superoxide dismutases that contribute to the protection of cowpea plants against oxidative stress. *African Journal of Biotechnology*, 6(17), pp.1982-1986.

Cai W, Shin DW, Chen K, Gheysens O, Cao Q, Wang SX, Gambhir SS and Chen X (2006) Peptide-Labeled Near-Infrared Quantum Dots for Imaging Tumor Vasculature in Living Subjects. *Nano Letters*, 6(4), pp.669-676.

Cao H, Jiang Y, Chen J, Zhang H, Huang W, Li L and Zhang W (2009) Arsenic accumulation in *Scutellaria baicalensis* Georgi and its effects on plant growth and pharmaceutical components. *Journal of Hazardous Materials*, 171, pp.508-513.

Chang HB, Lin CW and Huang HJ (2005) Zinc-induced cell death in rice (*Oryza sativa* L.) roots. *Plant Growth Regulation*, 46, pp.261-266.

Cheeseman JM (2007) Hydrogen Peroxide and Plant Stress: A Challenging Relationship. *Plant Stress*, 1, pp.4-15.

Chen A (2014) The Ethics of Nanotechnology. [Online] Available at: <http://www.scu.edu/ethics/publications/submitted/chen/nanotechnology.html> [Accessed on 9 February 2015].

Choi HS, Liu W, Misra P, Tanaka E, Zimmer JP, Ipe BI, Bawendi MG and Frangioni JV (2007) Renal clearance of quantum dots. *Nature Biotechnology*, 25(10), pp.1165-1170.

Chomoucka J, Drbohlavova J, Vaculovicova M, Businova P, Prasek J, Pekarek J and Hubalek J (2013) Study of Protein Conjugation with Different Types of CdTe Quantum Dots. *Nano and Micro Technologies*. ISBN 978-1-61208-303-2.

Ciarmiello LF, Woodrow P, Fuggi A, Pontecorvo G and Carillo P (2011) Plant Genes for Abiotic Stress. *Rijeka: InTech*. ISBN 978-953-307-394-1

Clemens S (2006) Toxic metal accumulation, responses to exposure and mechanisms of tolerance in plants. *Biochimie*, 88, pp.1707-1719.

Cohu, C.M. and Pilon, M., 2007. Regulation of superoxide dismutase expression by copper availability. *Physiologia Plantarum*, 129, pp.747-755.

Cooke MS, Evans MD, Dizdaroglu M and Lunec J (2003) Oxidative DNA damage: mechanisms, mutation, and disease. *The FASEB Journal*, 17(10), pp. 1195-1214.

Dalla Vecchia F, La Rocca N, Moro I, De Faveri S, Andreoli C and Rascio N (2005) Morphogenetic, ultrastructural and physiological damages suffered by submerged leaves of *Elodea canadensis* exposed to cadmium. *Plant Science*, 168, pp.329-338.

Deng DM, Shu WS, Zhang J, Zou HL, Lin Z, Ye ZH and Wong MH (2007) Zinc and cadmium accumulation and tolerance in populations of Sedum alfredii. *Environmental Pollution*, 147(2), pp.381-386.

Di Salvatore M, Carafa AM and Carratù G (2008) Assessment of heavy metals phytotoxicity using seed germination and root elongation tests: A comparison of two growth substrates. *Chemosphere*, 73, pp.1461-1464.

Dombrowski JE (2003) Salt stress activation of wound-related genes in tomato plants. *Plant Physiology*, 132, pp.2098-2107.

Draźkiewicz M, Skórzyńska-Polit E and Krupa Z (2003) Response of the ascorbate-glutathione cycle to excess copper in *Arabidopsis thaliana* (L.). *Plant Sciences*, 164, pp.195-202.

Draźkiewicz M, Skórzyńska-Polit E and Krupa Z (2004) Copper-induced oxidative stress and antioxidant defence in *Arabidopsis thaliana*. *BioMetals*, 17, pp.379-387.

Duan J, Song L and Zhan J (2009) One-Pot Synthesis of Highly Luminescent CdTe Quantum Dots by Microwave Irradiation Reduction and Their Hg^{2+} Sensitive Properties. *Nano Research*, 2, pp.61-68.

Ebbesen M and Jensen TG (2006) Nanomedicine: Techniques, Potentials, and Ethical Implications. *Journal of Biomedicine and Biotechnology*, 2006, pp.1-11.

Elstner EF (1991) Mechanisms of oxygen activation in different compartments of plant cells. In: EJ Pell, KL Steffen, eds. Active oxygen/oxidative stress and plant metabolism. Rockville: American Society of Plant Physiologists, pp.13-25.

Emamdoust A, Shayesteh SF and Marandi M (2013) Synthesis and characterization of aqueous MPA-capped CdS-ZnS core-shell quantum dots. *Indian Academy of Sciences*. 80(4), pp.713-721.

Emsley J (2001) Nature's Building Blocks: an A–Z guide to the elements. Oxford University Press. ISBN 978-0-19-850341-5.

Erasmus J (2013) Beneficiation 'an opportunity for BRICS'. [online] Available at: <http://www.southafrica.info/global/brics/mining-270313.htm> [Accessed on 22 May 2013].

Eriyarnremu GE, Asagba SO and Atoe K (2007) Lipid peroxidation, superoxide dismutase and mitochondria ATPases in the radicle of germinating beans (*Vigna unguiculata*) exposed to different doses of cadmium and lead. *Plant Archives*, 7, pp.39-45.

Fatoba PO and Emem UG (2008) Effects of Some Heavy Metals on Chlorophyll Accumulation in *Barbula lambarenensis*. *Ethnobotanical Leaflets*, 12, pp.776-783.

Feng RW, Wei CY, Tu SX, Wu FC and Yang LS (2009) Antimony accumulation and antioxidative responses in four fern plants. *Plant and Soil*, 317, pp.93-101.

Fenga R, Wei C, Tuc S, Dinga Y, Wanga R and Guoa J (2013) The uptake and detoxification of antimony by plants: A review. *Environmental and Experimental Botany*, 96, pp.28-34.

Fodor M, Hegedüs A and Stefanovits-Banyài É (2005) Zirconium induced physiological alterations in wheat seedlings. *Biologia Plantarum*, 49(4), pp.633-636.

Foyer CH and Noctor G (2005) Redox homeostasis and antioxidant signaling: A metabolic interface between stress perception and physiological responses. *Plant Cell*, 17, pp.1866-1875.

Foyer CH and Noctor G (2011) Ascorbate and Glutathione: The Heart of the Redox Hub. *Plant Physiology*, 155, pp.2-18.

Fridovich I (1986) Superoxide Dismutases. *Advances in Enzymology and Related Areas of Molecular Biology*, 58, pp.68-97.

Garg N and Manchanda G (2009) 'ROS generation in plants: boon or bane?'. *Plant Biosystems*, 143, pp.8-96.

Ghosh P, Han G, De M, Kim CK and Rotello VM (2008) Gold nanoparticles in delivery applications. *Advanced Drug Delivery Reviews*, 60, pp.1307-1315

Gichner T, Patkova Z, Szakova J and Demnerova K (2004) Cadmium induces DNA damages in tobacco roots, but no DNA damage, somatic mutations or homologous recombinations in tobacco leaves. *Mutatation Research*, 559, pp.49-57.

Gill SS and Tuteja N (2010) Reactive oxygen species and antioxidant machinery in abiotic stress tolerance in crop plants. *Plant Physiology and Biochemistry*, 48, pp.909-930.

Gokul A (2013) Impact of vanadium stress on physiological and biochemical in heavy metal susceptible and tolerant Brassicaceae. Unpublished MSc thesis. University of the Western Cape.
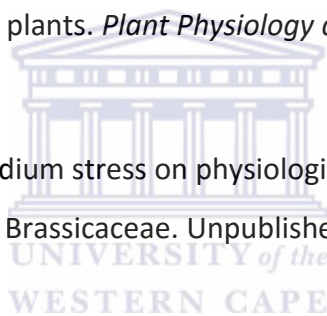
Gough DR and Cotter TG (2011) Hydrogen peroxide: a Jekyll and Hyde signalling molecule. *Cell Death and Disease*, 2, p.2.

Gratão PL, Polle A, Lea PJ and Azevedo RA (2005) Making the life of heavy metal-stressed plants a little easier. *Functional Plant Biology*, 32(6), pp.481-494.

Hall JL (2002) Cellular mechanisms for heavy metal detoxification and tolerance. *Journal of Experimental Botany*, 53, pp.1-11.

Hall JL and Williams LE (2003) Transition metal transporters in plants. *Journal of Experimental Botany*, 54(393), pp.2601-2613.

Halliwell B (2006) Reactive Species and Antioxidants. Redox Biology Is a Fundamental Theme of Aerobic Life. *Plant Physiology*, 141(2), pp.312-322.

Halliwell B and Gutteridge JM (1999) Free Radicals in Biology and Medicine. Oxford University Press.

Halliwell B, Clement M and Long L (2000) Hydrogen peroxide in the human body. *FEBS Letters,* 486, pp.10-13.

Hild WA, Breunig M, Goepferich A (2008) Quantum dots – Nano-sized probes for the exploration of cellular and intracellular targeting. *European Journal of Pharmaceutics and Biopharmaceutics*, 68, pp.153-168.

Jackson SMJ and Cooper JB (1998) An analysis of structural similarity in the iron and manganese superoxide dismutases based on known structures and sequences. *Biometals*, 11(2), pp.159-173.

Jimenez A, Hernandez JA, Pastori G, del Rio LA and Sevilla F (1998) Role of the ascorbate-glutathione cycle of mitochondria and peroxisomes in the senescence of pea leaves. *Plant Physiology*, 118, pp.1327-1335.

Kavuličová J, Kaduková J and Ivánová D (2012) The Evaluation of Heavy Metal Toxicity in Plants Using the Biochemical Tests. *Nova Biotechnologica et Chimica,* 11(2), pp.101-110.

Keyster M (2011) Nitric oxide-mediated signalling in legumes and its role in maize responses to salt treatment. Unpublished PhD thesis. University of Stellenbosch.

Kong Y, Akin AR, Francis KP, Zhang N, Troy TL, Xie H, Rao J, Cirillo SL and Cirillo JD (2011) Whole-body imaging of infection using fluorescence. *Current Protocols in Microbiology*, Chapter 2: Unit 2C.3.

Koramutla MK, Kaur A, Negi M, Venkatachalam P and Bhattacharya R (2014) Elicitation of jasmonate-mediated host defense in *Brassica juncea* (L.) attenuates population growth of mustard aphid *Lipaphis erysimi* (Kalt.). *Planta*, 240(1), pp.177-194.

Krämer U (2010) Metal Hyperaccumulation in Plants. *Annual Reviews in Plant Biology*, 61, pp.517-534.

Kuo WY, Huang CH, Liu AC, Cheng CP, Li SH, Chang WC, Weiss C, Azem A and Jinn TL (2013) CHAPERONIN 20 mediates iron superoxide dismutase (FeSOD) activity independent of its co-chaperonin role in Arabidopsis chloroplasts. *New Phytologist*, 197, pp.99-110.

Li CX, Feng SL, Shao Y, Jiang LN, Lu XY and Hou XL (2007) Effects of arsenic on seed germination and physiological activities of wheat seedlings. *Journal of Environmental Sciences*. 19, pp.725-732.

Liu X, Zhang S, Shan X and Zhu YG (2005) Toxicity of arsenate and arsenite on germination seedling growth and amylolytic activity of wheat. *Chemosphere*, 61, pp.293-301.

López-Millán AF, Ellis DR and Grusak MA (2005) Effect of zinc and manganese supply on the activities of superoxide dismutase and carbonic anhydrase in *Medicago truncatula* wild type and raz mutant plants. *Plant Science*, 168, 1015-1022.

Madhava Rao KV and Sresty TVS (2000) Antioxidative parameters in the seedlings of pigeonpea (*Cajanus cajan* (L.) Millspaugh) in response to Zn and Ni stresses. *Plant Science*, 157, pp.113-128.

Malar S, Vikram SS, Favas PJC and Perumal V (2014) Lead heavy metal toxicity induced changes on growth and antioxidative enzymes level in water hyacinths [*Eichhornia crassipes* (Mart.)]. *Botanical Studies*, 55(54), pp.1-11.

Marchiol L, Assolari L, Sacco P and Zerbi G (2004) Phytoextraction of heavy metals by canola (*Brassica napus*) and radish (*Raphanus sativus*) grown on multicontaminated soil. *Environmental Pollution*, 132, pp.21-27.

Marnett LJ (1999) Lipid peroxidation-DNA damage by malondialdehyde. *Mutation Research*, 424(1-2), pp.83-95.

Mattoussi H, Mauro JM, Goldman ER, Anderson GP, Sundar VC, Mikulec FV and Bawendi MG (2000) Self-Assembly of CdSe-ZnS Quantum Dot Bioconjugates Using an

Engineered Recombinant Protein. *Journal of American Chemical Society*, 122, pp.12142-12150.

Mattoussi H, Mauro JM, Goldman ER, Green TM, Anderson GP, Sundar VC and Bawendi MG (2001) Bioconjugation of Highly Luminescent Colloidal CdSe–ZnS Quantum Dots with an Engineered Two-Domain Recombinant Protein. *Physica Status Solidi*, 224(1), pp.277-283.

McCarthy TS (2011) The impact of acid mine drainage in South Africa. *South African Journal of Science*, 107(6), pp.1-7.

Mhamdi A, Queval G, Chaouch S, Vanderauwera S, Van Breusegem F and Noctor G (2010) Catalase function in plants: a focus on *Arabidopsis* mutants as stress-mimic models. *Journal of Experimental Botany*, 61(15), pp.4197-4220.

Miriyala S, Spasojevic I, Tovmasyan A, Salvemini D, Vujaskovic Z, St. Clair D and Batinic-Haberle I (2012) Manganese superoxide dismutase, MnSOD and its mimics. *Biochimica et Biophysica Acta*, 1822(2012), pp.794-814.

Mittler R and Zilinskas BA (1992) Molecular cloning and characterization of a gene encoding pea cytosolic ascorbate peroxidase. *Journal of Biological Chemistry*, 267, pp.21802-21807.

Mohamed N (2000) At the crossroads: land and agrarian reform in South Africa into the 21st century. Cape Town: University of the Western Cape. ISBN 1-86808-467-1.

Mohammed SA and Ahmad (2009) Selective Extraction of Zirconium from Various Samples and Subsequent Spectrophotometric Determination with Eriochrome Cyanine R Reagent. *Rafidain Journal of Science*, 20(2), pp.74-83.

Montecinos V, Guzmán P, Barra V, Villagrán M, Muñoz-Montesino C, Sotomayor K, Escobar E, Godoy A, Mardones L, Sotomayor P, Guzmán C, Vásquez O, Gallardo V, van Zundert B, Bono MR, Oñate SA, Bustamante M, Cárcamo JG, Rivas CI and Vera JC (2007) Vitamin C Is an Essential Antioxidant That Enhances Survival of Oxidatively

Stressed Human Vascular Endothelial Cells in the Presence of a Vast Molar Excess of Glutathione. *The Journal of Biological Chemistry*, 282, pp.15506-15515.

Mullineaux PM and Rausch T (2005) Glutathione, photosynthesis and the redox regulation of stress-responsive gene expression. *Photosynthesis Research*, 86, pp.459-474.

Mylonas C and Kouretas D (1999) Lipid peroxidation and tissue damage. *In Vivo*, 13(3), pp.295-309.

Myouga F, Hosoda C, Umezawa T, Iizumi H, Kuromori T, Motohashi R, Shono Y,Nagata N, Ikeuchi M and Shinozakia K (2008) A Heterocomplex of Iron Superoxide Dismutases Defends Chloroplast Nucleoids against Oxidative Stress and Is Essential for Chloroplast Development in *Arabidopsis*. *The Plant Cell*, 20, pp.3148-3162.

Noctor G and Foyer CH (1998) 'A re-evaluation of the ATP: NADPH budget during C3 photosynthesis. A contribution from nitrate assimilation and its associated respiratory activity?'. Journal of Experimental Botany. 49, pp.1895-1908.

Noctor G, Mhamdi A, Chaouch S, Han Y, Nuekermans J, Marquez-Garcia B, Queval G and Foyer CH (2012) Glutathione in plants: an integrated overview. *Plant, Cell & Environment*, 35(2), pp.454-484.

Norris L (2013) Necrosis Plant Diseases. *SFGate* [online] Available at: <http://homeguides.sfgate.com/necrosis-plant-diseases-39504.html> [Accessed 2 January 2014].

Ozturk F, Duman F, Leblebici Z and Temizgul R (2010) Arsenic accumulation and biological responses of watercress (*Nasturtium officinale* R. Br.) exposed to arsenite. *Environmental and Experimental Botany*, 69, pp.167-174.

Pahlsson AB (1989) Toxicity of heavy metals (Zn, Cu, Cd, Pb) to vascular plants. *Water, Air, and Soil Pollution*, 47, pp.287-319.

Palmer, AR and Ainslie, AM (2005) 'Grasslands of South Africa'. In: JM Suttie, SG Reynolds and C Batello eds. Grasslands of the world. Plant production and protection series 34, Food and Agriculture Organization of the United Nations, Rome, pp. 77-120.

Palmer T and Ainslie A (2006) Country Pasture/Forage Resource Profiles: South Africa. [online] Available at: <http://www.fao.org/ag/AGP/AGPC/doc/Counprof/PDF%20files/South Africa_English.pdf> [Accessed 14 February 2015].

Pickering IJ, Prince RC, George MJ, Smith RD, George GN and Salt DE (2000) Reduction and coordination of arsenic in Indian mustard. *Plant Physiology*, 122, pp.1171-1177.

Porter JR and Richard P (1981) Inhibition of Nitrogen Fixation in Alfalfa by Arsenate, Heavy Metals, Fluoride, and Simulated Acid Rain. *Plant Physiology*, 68, pp.143-148.

Prasad KVSK, Saradhi PP and Sharmila, P (1999) Concerted action of antioxidant enzymes and curtailed growth under zinc toxicity in *Brassica juncea*. *Environmental and Experimental Botany*, 42, pp.1-10.

Puntarulo S, Sánchez RA and Boveris A (1988) Hydrogen peroxide metabolism in soybean embryonic axes at the onset of germination, Plant Physiology, 86, pp.626-630.

Quan LJ, Zhang B, Shi WW and Li HY (2008) Hydrogen peroxide in plants: a versatile molecule of the reactive oxygen species network. *Journal of Integrative Plant Biology*, 50(1), pp.2-18.

Queval G and Noctor G (2007) A plate reader method for the measurement of NAD, NADP, glutathione, and ascorbate in tissue extracts: Application to redox profiling during *Arabidopsis rosette* development. *Analytical* Biochemistry, 363(1), pp.58-69.

Rahman H, Sabreen S, Alam S, Kawai S (2005) Effects of nickel on growth and composition of metal micronutrients in barley plants grown in nutrient solution. *Journal of Plant Nutrition*, 28, pp.393-404.

Rana S, Bajaj A, Mout R, Rotello VM (2012) Monolayer coated gold nanoparticles for delivery applications. *Advanced Drug Delivery Reviews*, 64, pp.200-216.

Rascioa N and Navari-Izzob F (2011) 'Heavy metal hyperaccumulating plants: How and why do they do it? And what makes them so interesting?. *Plant* Science, 180, pp.169-181.

Rascioa N, Dalla Vecchiaa F, La Roccaa N, Barbatob R, Paglianob C, Raviolob M, Gonnellic C and Gabbrielli R (2008) Metal accumulation and damage in rice (*cv.* Vialone nano) seedlings exposed to cadmium. *Environmetal and Experimental Botany*, 62, pp.267-278.

Reeves RD (2006) Hyperaccumulation of trace elements by plants. In: JL Morel, G Echevarria, N Goncharova, eds. Phytoremediation of Metal-Contaminated Soils. *NATO Science Series: IV: Earth and Environmental Sciences*, New York: Springer, pp.1-25.

Roosens N, Verbruggen N, Meerts P, Ximenez-Embun P and Smith JA (2003) Natural variation in cadmium tolerance and its relationship to metal hyperaccumulation for seven populations of *Thlaspi caerulescens* from western Europe. *Plant, Cell and Environment*, 26, pp.1657-1672.

Russo M, Sgherri C, Izzo R and Navari-Izzo F (2008) *Brassica napus* subjected to copper excess: Phospholipases C and D and glutathione system in signalling. *Environmental and Experimental Botany*, 62, pp.238-246.

Sanevas N, Sunohara Y and Matsumoto H (2007) Characterization of reactive oxygen species involved oxidative damage in Hapalosiphon species crude extract-treated wheat and onion roots. *Weed Biology and Management*, 7, pp.172-177.

Schützendübel A and Polle A (2002) Plant responses to abiotic stress: heavy metal-induced oxidative stress and protection by mycorrhization. *Journal of Experimental Botany*, 53(372), pp.1351-1365.

Seckin B, Turkan I, Sekmen AH and Ozfidan C (2010) The role of antioxidant defense systems at differential salt tolerance of *Hordeum marinum* Huds. (sea barleygrass) and

Hordeum vulgare L. (cultivated barley). *Environmental and Experimental Botany*, 69, pp.76-85.

Shahab Jalali-e-Emam SM, Alizadeh B, Zaefizadeh M, Zakarya RA and Khayatnezhad M (2011) Superoxide Dismutase (SOD) Activity in NaCl Stress in Salt-Sensitive and Salt Tolerance Genotypes of Colza (*Brassica napus L*.). *Middle-East Journal of Scientific Research*, 7(1), pp.7-11.

Shakya K, Chettri MK and Sawidis T (2008) Impact of Heavy Metals (Copper, Zinc, and Lead) on the Chlorophyll Content of Some Mosses. *Archives of Environmental Contamination and Toxicology*, 54(3), pp.412-421.

Shao H, Chu L, Lu Z and Kang C (2008) Primary antioxidant free radical scavenging and redox signaling pathways in higher plant cells. *International Journal of Biological Science*s, 4(1), pp.8-14.

Sharma P, Jha AB, Dubey RS and Pessarakli M (2012) Reactive Oxygen Species, Oxidative Damage, and Antioxidative Defense Mechanism in Plants under Stressful Conditions. *Journal of Botany*, 2012, p26.

Sharma SS and Dietz KJ (2008) The relationship between metal toxicity and cellular redox imbalance. *Trends in Plant Science*, 14(1), pp.43-50.

Shen M, Jia W, You Y, Hu Y, Li F, Tian S, Li J, Jin Y and Han D (2013) Luminescent properties of CdTe quantum dots synthesized using 3-mercaptopropionic acid reduction of tellurium dioxide directly. *Nanoscale Research Letters*, 8(253), pp.1-6.

Shi D, Guo Z and Bedford N (2015) Nanomaterials and Devices: A volume in Micro and Nano Technologies. Oxford: Elsevier.

Smirnoff N (2005) Ascorbate, tocopherol and carotenoids: metabolism, pathway engineering and functions. In: N Smirnoff, eds. Antioxidants and Reactive Oxygen Species in Plants. Oxford: Blackwell Publishing Ltd, pp.53-86.

Soenen SJ, Manshian BB, Aubert T, Himmelreich U, Demeester J, De Smedt SC, Hens Z and Braeckmans K (2014) Cytotoxicity of cadmium-free quantum dots and their use in cell bioimaging. *Chemical Research in Toxicology*, 27(6), pp.1050-1059.

Statistics South Africa (2011) Mid-year population estimates. [online] Available at: <http://www.statssa.gov.za/publications/P0302/P03022011.pdf> [Accessed 22 May 2013].

Stephan D, Slabber C, George G, Ninov V, Francis KP and Burger JT (2011) Visualization of plant viral suppressor silencing activity in intact leaf lamina by quantitative fluorescent imaging. *Plant Methods*, 7(25), pp.1-9.

Takahashi MA and Asada K (1983) Superoxide anion permeability of phospholipid membranes and chloroplast thylakoids. *Archives of Biochemistry and Biophysics*, 226(2), pp.558-566.

Tani FH and Barrington S (2005) Zinc and copper uptake by plants under two transpiration rates. Part II. Buckwheat (*Fagopyrum esculentum* L.). *Environmental Pollution*, 138, pp.548-558.

Thanan R, Oikawa S, Hiraku Y, Ohnishi S, Ma N, Pinlaor S, Yongvanit P, Kawanishi S and Murata M (2015) Oxidative stress and its significant roles in neurodegenerative diseases and cancer. *International Journal of Molecular Sciences*, 16, pp.193-217.

Tsang EWT, Bowler C, Herouart D, Van CW, Villarroel R, Genetello C, Van MM and Inze D (1991) Differential regulation of superoxide dismutase in plants exposed to environmental stress. *Plant Cell*, 3, pp.783-792.

Turrens JF (2003) Mitochondrial formation of reactive oxygen species. *Journal of Physiology*, 552.2, pp.335-344.

Tuteja N, Ahmad P, Panda BB and Tuteja R (2009) Genotoxic stress in plants: shedding the light of DNA damage, repair and DNA repair helicases. *Mutation Research*, (2-3), pp.134-149.

Tuteja N and Tuteja R (2001) Unraveling DNA repair in human: molecular mechanisms and consequences of repair defect. *Critical Reviews in Biochemistry and Molecular Biology*, 36(3), pp.261-290.

Van Breusegem F and Dat JF (2006) Reactive Oxygen Species in Plant Cell Death. *Plant Physiology*, 141, pp.384-390.

Velcheva I, Petrova S, Dabeva V and Georgiev D (2012) Eco-physiological study on the influence of contaminated waters from the Topolnitza River catchment area on some crops. *Ecologia Balkanica*, 4(2), pp.33-41.

Verbruggen N, Hermans C and Schat H (2009). Molecular mechanisms of metal hyperaccumulation in plants. *New Phytologist,* 181, pp.759-776.

Verma S and Dubey RS (2003) Lead toxicity induces lipid peroxidation and alters the activities of antioxidant enzymes in growing rice plants. *Plant Science*, 164, pp.645-655.

Vickers CE, Gershenzon J, Lerdau MT and Loreto F (2009) A unified mechanism of action for volatile isoprenoids in plant abiotic stress. *Nature Chemical Biology*, 5, pp.283-291.

Vranová E, Atichartpongkul S, Villarroel R, Van Montagu M, Inze D and Van Camp W (2002) Comprehensive analysis of gene expression in Nicotiana tabacum leaves acclimated to oxidative stress. *PNAS*, 99, pp.870-875.

Wahsha M, Bini C, Fontana S, Wahsha A and Zilioli D (2012) Toxicity assessment of contaminated soils from a mining area in Northeast Italy by using lipid peroxidation assay. *Journal of Geochemical Exploration*, 113, pp.112-117.

Wang W, Vinocur B, Altman A (2003) Plant responses to drought, salinity and extreme temperatures: towards genetic engineering for stress tolerance. *Planta*, 218(1), pp.1-14.

Wojtaszek P (1997) Oxidative burst: an early plant response to pathogen infection. *Biochemical Journal*, 322, pp.681-692.

Wong M (2006) Mature Leaf Chlorosis and Necrosis. *College of Tropical Agriculture and Human Resources*, L15, pp.1.6.

Xiang C, Werner BL, Christensen EM and Oliver DJ (2001) The biological functions of glutathione revisited in Arabidopsis transgenic plants with altered glutathione levels. *Plant Physiology*, 126, pp.564-574.

Xuan Tham L, Nagasawa N, Matsuhashi S, Ishioka NS, Ito T and Kume T (2001) Effect of radiation-degraded chitosan on plants stressed with vanadium. *Radiation Physics and Chemistry*, 61(2), pp.171-175.

Yadav SK (2010) Heavy metals toxicity in plants: An overview on the role of glutathione and phytochelatins in heavy metal stress tolerance of plants. *South African Journal of Botany*, 76, pp.167-179.

Yamamoto Y, Kobayashi Y and Matsumoto H (2001) Lipid Peroxidation Is an Early Symptom Triggered by Aluminium, But Not the Primary Cause of Elongation Inhibition in Pea Roots. *Plant Physiology*, 125, pp.199-208.

Yan C, Tang F, Li L, Li H, Huang X, Chen D, Meng X and Ren J (2010) Synthesis of Aqueous CdTe/CdS/ZnS Core/shell/shell Quantum Dots by a Chemical Aerosol Flow Method. *Nanoscale Research Letters*, 5, pp.89-194.

Yu Y, Zhang K, Li Z and Sun S (2012) Synthesis and luminescence characteristics of DHLA-capped PbSe quantum dots with biocompatibility. *Optical Materials*, 34, pp.793-798.

Zehra SS, Arshad M, Mahmood T and Waheed A (2009) Assessment of heavy metal accumulation and their translocation in plant species. *African Journal of Biotechnology*, 8(12), pp.2802-2810.

Zhang F, Wang Y, Lou Z and Dong J (2007) Effect of heavy metal stress on antioxidative enzymes and lipid peroxidation in leaves and roots of two mangrove plant seedlings (*Kandelia candel* and *Bruguiera gymnorrhiza*). *Chemosphere,* 67, pp.44-50.

Zhou X, Carranco R, Vitha S and Hall TC (2005) The dark side green fluorescent protein. *The New Phytologist*, 168, pp.313-322
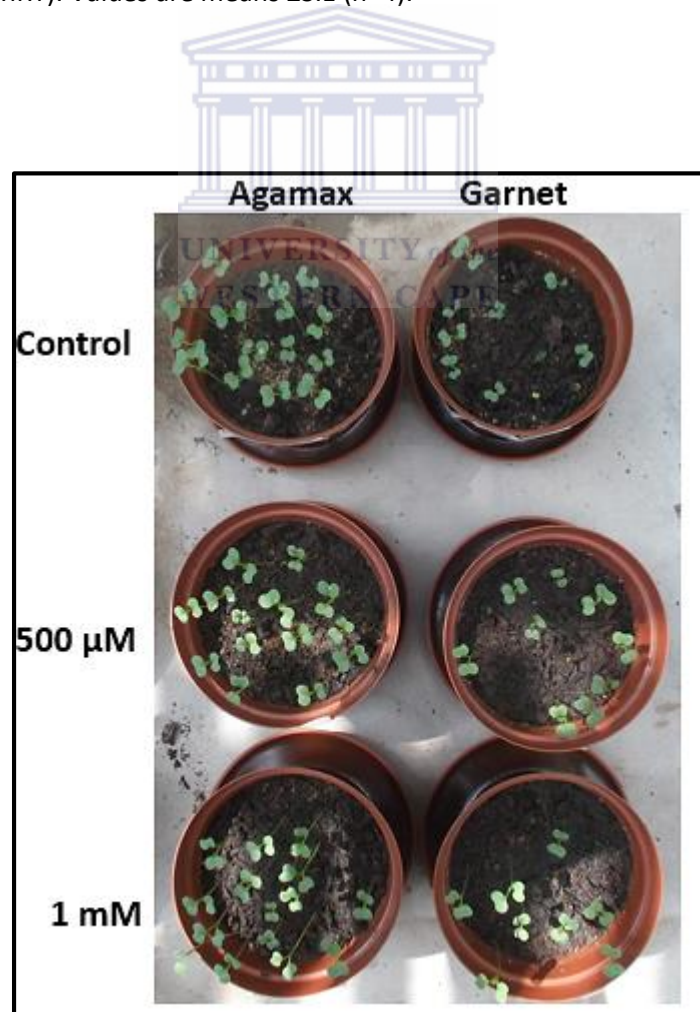
Supplementary Table 1: Germination percentages of canola genotypes due to zirconium treatment.

Concentration of Zr	Agamax	Garnet
Control	100% ± 0.003[a]	73% ± 0.046[a]
500 μM	93% ± 0.88[b]	68% ± 1.45[b]
1 mM	93% ± 1.20[c]	53% ± 1.86[c]

Different letters indicate significant difference between means at $P<0.05$ (DMRT). Values are means ±S.E (n=4).

Supplementary Figure 1: Effect of zirconium treatment on the germination of two canola genotypes.